Graduate School ETD Form 9
(Revised 12/07)

PURDUE UNIVERSITY
GRADUATE SCHOOL
Thesis/Dissertation Acceptance

This is to certify that the thesis/dissertation prepared

By Jie Xue

Entitled Optimal Power Control of a Wind Turbine Power Generation System

For the degree of Master of Science in Electrical and Computer Engineering

Is approved by the final examining committee:

Yaobin Chen
Chair

Lingxi Li

Steven Rovnyak

To the best of my knowledge and as understood by the student in the *Research Integrity and Copyright Disclaimer (Graduate School Form 20)*, this thesis/dissertation adheres to the provisions of Purdue University's "Policy on Integrity in Research" and the use of copyrighted material.

Approved by Major Professor(s): Yaobin Chen

Approved by: Yaobin Chen 07/26/2011
Head of the Graduate Program Date

Graduate School Form 20
(Revised 9/10)

PURDUE UNIVERSITY
GRADUATE SCHOOL

Research Integrity and Copyright Disclaimer

Title of Thesis/Dissertation:

Optimal Power Control of a Wind Turbine Power Generation System

For the degree of Master of Science in Electrical and Computer Engineering

I certify that in the preparation of this thesis, I have observed the provisions of *Purdue University Executive Memorandum No. C-22*, September 6, 1991, *Policy on Integrity in Research.**

Further, I certify that this work is free of plagiarism and all materials appearing in this thesis/dissertation have been properly quoted and attributed.

I certify that all copyrighted material incorporated into this thesis/dissertation is in compliance with the United States' copyright law and that I have received written permission from the copyright owners for my use of their work, which is beyond the scope of the law. I agree to indemnify and save harmless Purdue University from any and all claims that may be asserted or that may arise from any copyright violation.

Jie Xue
_____
Printed Name and Signature of Candidate

07/25/2011
_____
Date (month/day/year)

*Located at http://www.purdue.edu/policies/pages/teach_res_outreach/c_22.html

OPTIMAL POWER CONTROL OF A WIND TURBINE POWER GENERATION SYSTEM

A Thesis

Submitted to the Faculty

of

Purdue University

by

Jie Xue

In Partial Fulfillment of the

Requirements for the Degree

of

Master of Science in Electrical and Computer Engineering

August 2011

Purdue University

Indianapolis, Indiana

To my family.

ACKNOWLEDGMENTS

I would like to gratefully acknowledge my thesis advisor, Dr. Yaobin Chen, for his assistance, guidance, and supervision during the entire course of this research and thesis work. Dr. Chen generously shared with me his research experience and directed me towards perfection in every detail, for which I am always thankful. I would like to thank my advisor committee member Dr. Steven Rovnyak and Dr. Lingxi Li for their time and insight during the completion of this thesis. I would also like to thank Mrs. Valerie Lim Diemer and Mrs. Sherrie Tucker for assisting me in formatting this thesis.

TABLE OF CONTENTS

Page

LIST OF FIGURES

Figure Page

ABSTRACT

Xue, Jie. M.S.E.C.E, Purdue University, August 2011. Optimal Power Control of A Wind Turbine Power Generation System. Major Professor: Yaobin Chen.

This thesis focuses on optimization of wind power tracking control systems in order to capture maximum wind power for the generation system. In this work, a mathematical simulation model is developed for a variable speed wind turbine power generation system. The system consists a wind turbine with necessary transmission system, and a permanent magnet synchronous generator and its vector control system. A new fuzzy based hill climbing method for power tracking control is proposed and implemented to optimize the wind power for the system under various conditions. Two existing power tracking control methods, the tip speed ratio (TSR) control method and the speed sensorless control method are also implemented with the wind power system. The computer simulations with a 5 KW wind power generation system are performed. The results from the proposed control method are compared with those obtained using the two existing methods. It is illustrated that the proposed method generally outperforms the two existing methods, especially when the operating point is far away from the maximum point. The proposed control method also has similar stable characteristic when the operating point is close to the peak point in comparison with the existing methods. The proposed fuzzy control method is computationally efficient and can be easily implemented in real-time.

1. INTRODUCTION

1.1 Background

Due to its environmental, social and economical benefits, as shown in Fig 1.1 the wind power industry has been growing significantly in the past 10 years. In 2009, the worldwide wind power capacity has increased 31.7% or (38,310 MW). Because of the rapid growth, the world total wind power capacity has attained 159,213 MW. The wind energy capacity in the US increased 9,922 MW in 2009. And the installed capacity has added up to the amount of 35,159 MW. Roughly speaking, the electricity generated by wind in the US can meet the electricity requirement of about 15 million homes and save approximate 1500 million tons of carbon emissions, the same as taking nearly 260 million cars off the road annually [1].

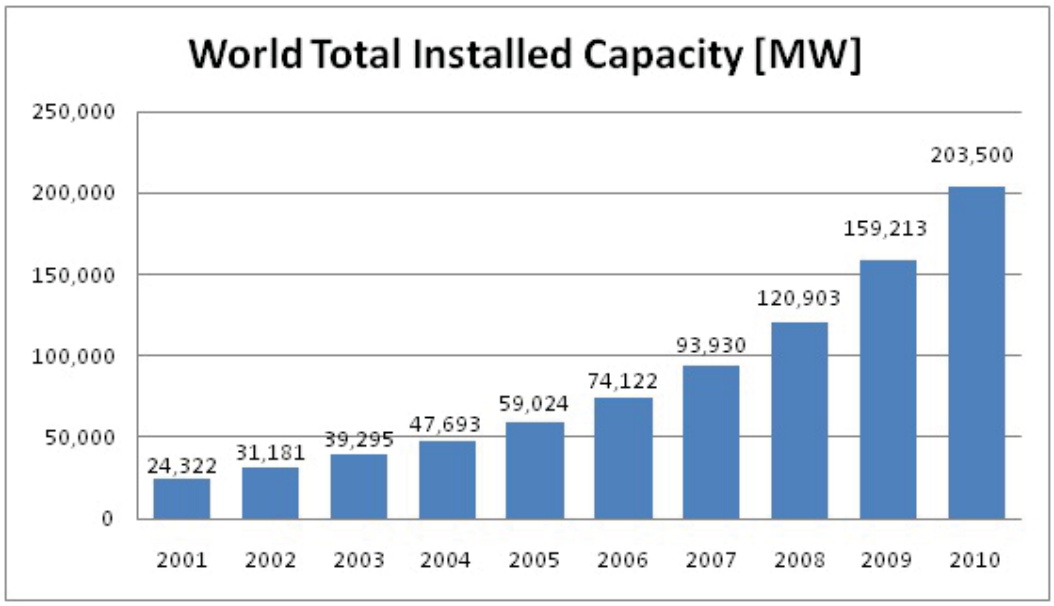

Fig. 1.1. World total installed capacity (2001 to 2010)

As a result of wind farms installed in New York, Texas and California, the US has gained the first rank of wind power capacity in the world, with China (26,010 MW) and Germany (25,777 MW) following close. As shown in Fig 1.2, USA and China are the top two countries of new installed wind power capacity in 2009. They share the new capacity of 23,777 MW, 61.9% of the world total [2].

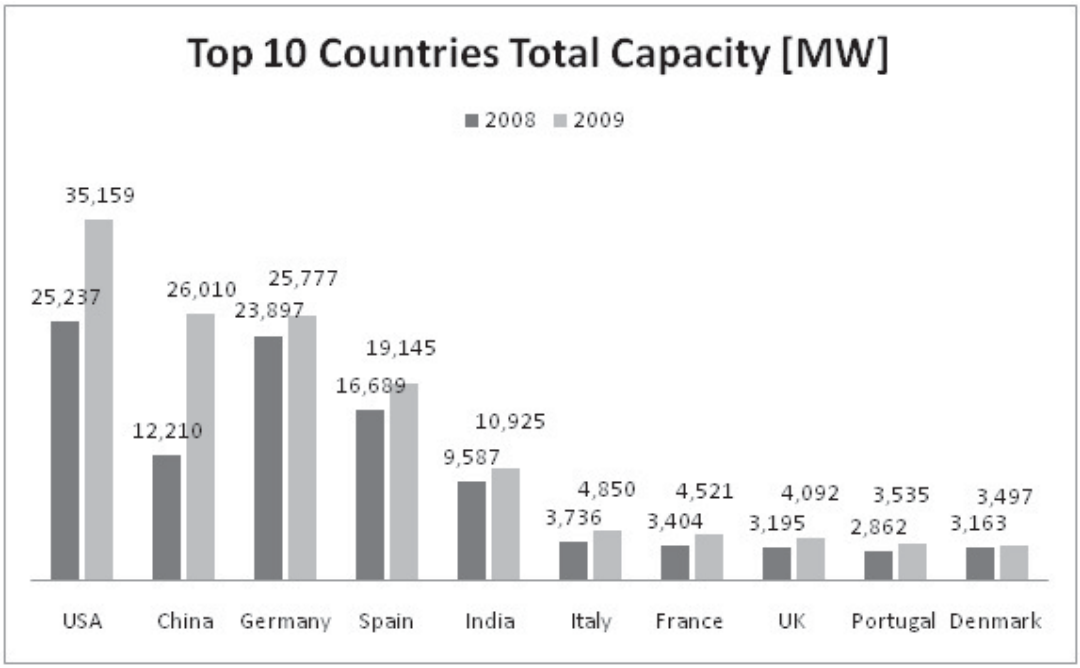

Fig. 1.2. Top 10 countries total capacity

Many countries have long term plans for developing wind power in the future. The target of the US is to provide 20% total electricity by wind energy in 2030. In addition, China, India, German, Spain, Italy and France have similar plans to build large and medium-small wind farms [3].

As wind resource has an inherent characteristic of randomness, the wind power would have a potential unpredictable influence on the grid. The influence is acceptable when the contribution rate is less than 3%. However, enormous risk may occur when the contribution rate is beyond 8% [4]. The cases in Germany showed that by

using small and median wind machine, the risk can be effectively alleviated. Like solar panels, small roof top wind machines could be widely used in distributed power system [5]. In this kind of smart power system, wind power does not connect with long distance grid transmission system. The electricity is only generated and consumed through user side grid [6].

1.2 Brief Historical Review of Wind Power Generation

It is a long history since human started to use wind resource. In 500 BC, the ancient Egyptians transported by sail boats on the Nile. And the vertical wind mill appeared on the plateau of Afghanistan for irrigation in about 7th century BC.

There are historical documents in China and Persia, recorded the application of vertical-axis wind mill and wind pump. However, different materials were chosen to build the sail surface, Chinese preferred canvas while Persian preferred bundle of reed. Influenced by East Expeditions of Crusades, the Persian vertical wind mill soon spread to the littoral countries of the Mediterranean, then to the other countries in Europe. In the expand process, the type has evolved from vertical to horizontal. The reasons for this change are remain suspense. One possible reason is that the European craftsmen use the same technique model of hydro turbine which is also horizontal. Another potential reason is that there is stable wind direction in Persia while the wind direction in Europe is variable in full angles. Perhaps, the improvement is to make the wind mill adapt the wind regime better.

The techniques of wind mill continued to develop in the 12th and 16th century. At the end of 19th century, the typical Dutch's wind mill has a height of 30 m with a rotor diameter of 25 m. Wind turbine are used widely at that time, not only for grinding but also for pumping water to exhaust lakes and marshland. Till 1800s, there are more than 20,000 wind mill built in France. While in Holland, wind provided approximate 90 % of total energy. However, the extensively use of steam engine led to abandon of thousands wind mills.

As the wind mills were vanishing in Europe, the colonist took them to North America to pump water for cattle. This kind of American wind mills has mechanical automatic control that the direction would change under the control of a fin. The installed wind mills capacity in American reached the peak between 1920s and 1930s with a total amount of about 60,000.

The first wind power system was built in Cleveland, OH by Charles F. Brush in1888. The rotor was formed by 144 wooden blades with a diameter of 17 meters which was placed on a tower 18 meters high. The pulley gear transmission with the ratio 50:1 was coupled with a 12 KW DC generator placed in the basement under the tower.

In the First and the Second World War, Danish engineers have made some technique improvement of wind power. The wind turbine made by F.L Smidth Company in 1942 was regard as the leading pioneer of modern wind power as the aerodynamics was first used in blade design. Meanwhile, a few experimental units were built in America and Germany. Although these early wind turbines has gained some achievements in blade aerodynamic design and yawing system, the interest of wind power still faded down after Second World War. Only some small units were still used in remote area for power supply.

The oil crisis in 1970s evoked the great interest of wind energy. Many stagnant projects got financial support and stopped researches were continued. The institutes and enterprisers in Germany, American, Sweden and Denmark started to build MW-sized prototype wind power system. However, these attempts are unsuccessful due to a series of problems on pitch control. Some countries suspended the support but the wind energy research in Denmark survived by special government support development projects [7].

After ten years of exploration and experiment, the commercial wind turbine began to release in the early 1980s. In 1978 the US Department of Energy published the PURPA (Public Utility Regulatory Policies Act) which allowed individuals to set up wind machines and connect them with the grid. This policy gave tremendous opportu-

nities to the medium-small wind machine. Although the market prospect is exciting, the technique defects of material fatigue strength and load control delayed the wind power's pace forward. With the improvement of technology, in late 1980s, the wind turbine capacity increased to 250 to 300 KW per unit. The market demand was also stimulated by governments' subsidy. However, in industrial application wind turbine can seldom reach the designed life cycle of 20 years. Wind power was uncompetitive without the governments' support at that time.

In 1990s, benefiting from the tax policy of European countries, especially Germany, the wind power capacity began to grow rapidly. As the market scale expanded, the wind turbine technique got mature gradually after 20 years of failure experiments. The single unit capacity has jumped to MW level at the end of 20th century [8]. The most popular wind power unit is 1.5 MW onshore and 3 MW offshore and higher power level experimental units are built for offshore usage [9].

With the large scale application of wind power, there occurs many problems to be solved. The materials of blades and tower need to be light, tough and tensile especially offshore wind turbines. The grid connect-in surge in weak regional power grid should be avoided. The research of wind power plants macrositing and micrositing can go deeper. The power tracking strategies could be optimized on maximum power point tracking (MPPT) and power limit for higher efficiency. This thesis focuses on MPPT problems by using optimization techniques [10].

1.3 System Configurations of Wind Power Generation

Variable speed wind power system is quite popular in the past decades. Compared with constant speed wind machine, variable speed wind machine could operate in larger wind speed range. Wind resource changes from time to time, therefore, a maximum power point tracking power control system is needed to follow the change and capture the maximum energy from the wind.

1.3.1 Variable Speed Wind Energy System

Variable speed wind machine is quite popular nowadays for both KW-sized and MW-sized. Compared with installed speed wind machines, variable speed wind turbines generate 10-15% more power; have lower stress on the mechanical components especially the blades and shafts; cause less power fluctuation and less influence on the grid [11].

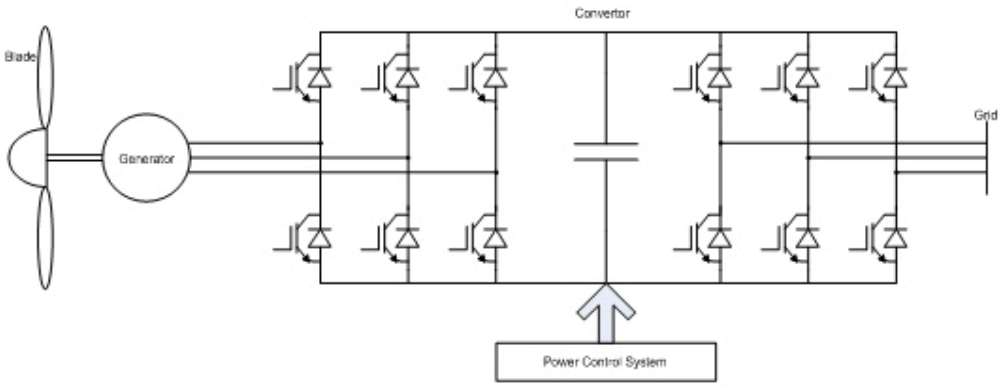

Fig. 1.3. Variable speed wind energy system

Fig 1.3 shows the structure of a variable speed wind energy system. A typical wind energy system is mainly comprised of blades, generator, power control system and a back to back PWM convertor. The blades transform the wind energy into rotational mechanical energy so as to drive the generator. The electricity generated is variable frequency and variable voltage which cannot feed into the grid directly. An AC/DC and DC/AC converter is necessary to change the electricity into constant frequency and constant voltage with synchronous phase angle so that grid connect would be possible. The converter is under the control of the power tracking system. This control system has two main functions that is maximum power tracking and maximum power limit. The AC/DC circuit is called generator side converter which accomplishes the power control and maintains DC link voltage. The DC/AC circuit is named grid side converter which is a general PWM voltage rectifier [12].

Gearbox is optional nowadays, for direct drive wind turbines, gearbox can be removed for higher power density and transmission efficiency. Both synchronous generator and asynchronous generator are chosen for wind energy system. At present, permanent magnet synchronous machine (PMSM) is used widely in small and median wind machine, especially in direct drive wind machine. The recent trend is that multi-pole PMSM use in large scale wind power such as 1.5 MW which operates at a relative low wind speed. The double-fed induction generator (DFIG) is also widely used because constantly power would be provided at a large range of wind speed [13].

1.3.2 Maximum Power Point Tracking Principle

Variable speed wind turbine can operate effectively in a wide range of wind speed. There is rated power P_{rated} at the rated wind speed V_{rated} for each wind turbine which is mainly decided by mechanical characteristic.

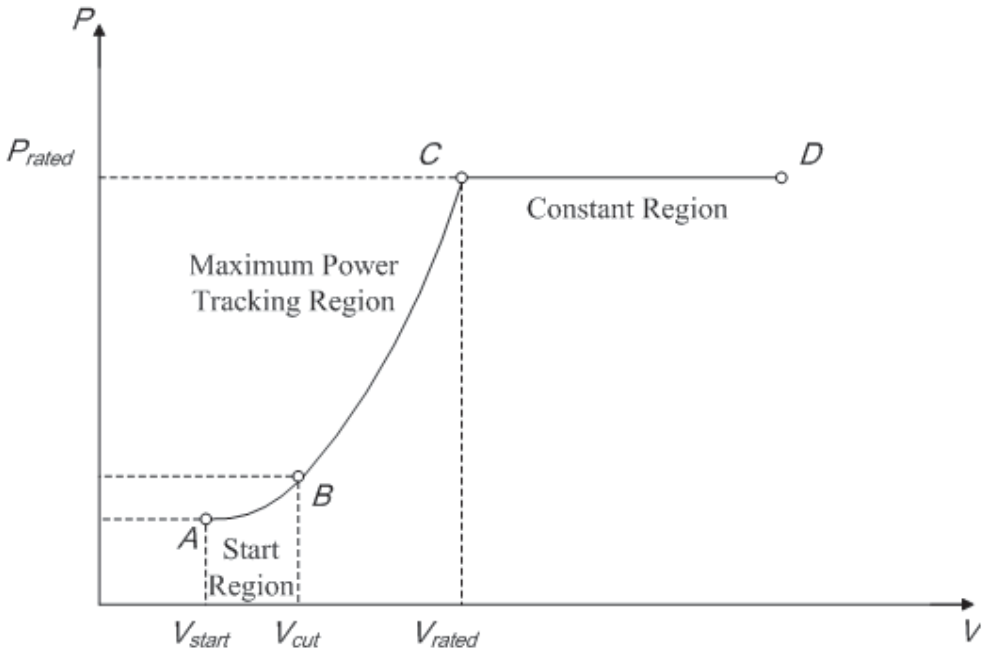

Fig. 1.4. Mechanical output power VS wind speed

As shown in Fig 1.4 the rated speed divides the working range into two different regions, the below rated wind speed region and the above rated wind speed region. The region above rated wind speed is also called constant power region because the power is limited for mechanical and electrical protection. And there has a cut-in speed V_{cut} in below rated wind speed region which is impacted by mechanical and power electrical design. It is only at the cut-in speed that the power system joins the grid and begins to output power. The cut-in speed divides the below rated region into maximum power tracking region and start region. The start region is from start wind speed V_{start} to cut-in speed. Fig 1.4 shows the relationship between total electromagnetic power and wind speed V_{cut}. Fig 1.5 describes the relationship between electromagnetic power and generator rotational speed. $\omega_{m\_\min}$ is the lowest rotational speed for wind turbine, the generator would be off the grid if rotational speed is lower. The generator synchronous speed is ω_{m_syn} while the maximum rotational speed is $\omega_{m\_\max}$.

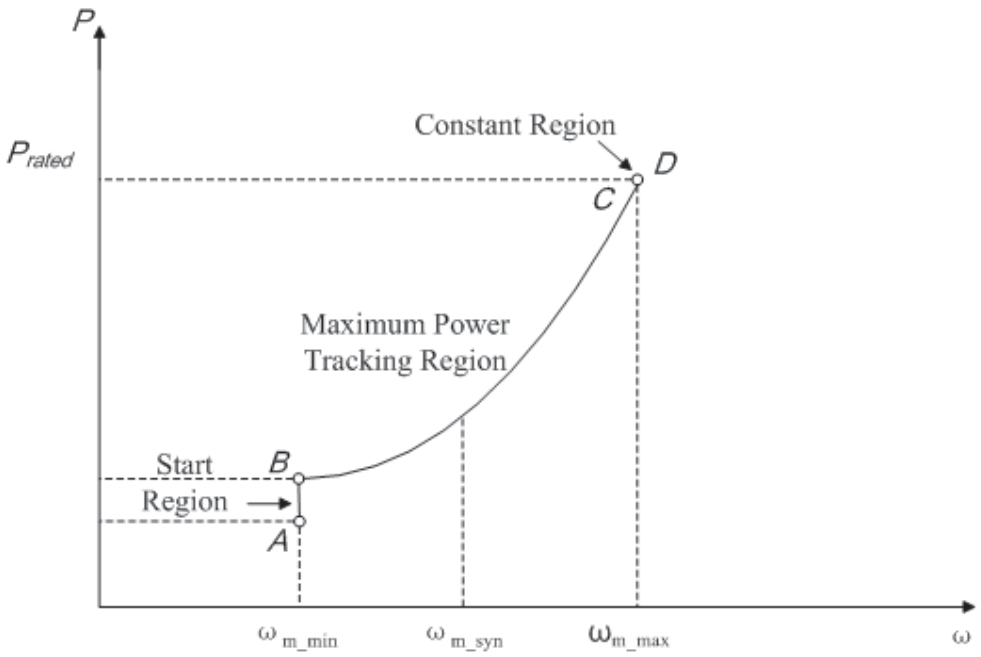

Fig. 1.5. Generator electromagnetic power VS rotation speed

The maximum power tracking region is the BC curve in Fig 1.4 and Fig 1.5. In this region, the power output is only affected by generator rotational speed. The ultimate goal of MPPT is to keep the wind machine operates on optimal curve, shown as the P_{opt} curve in Fig 1.6 [14].

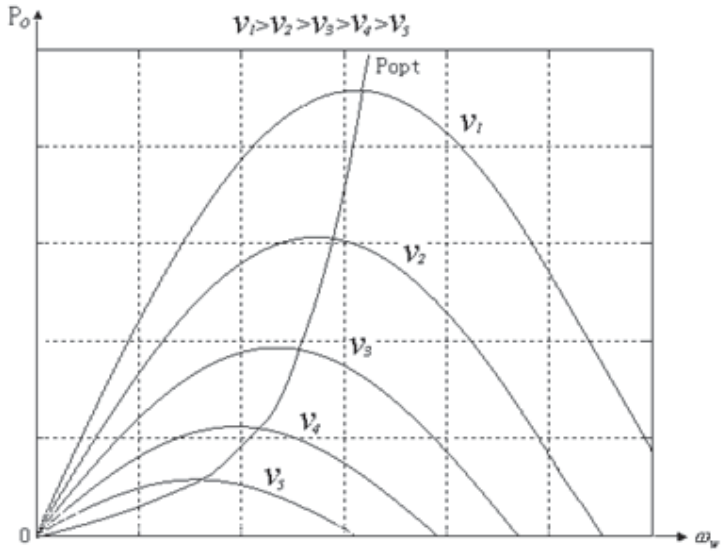

Fig. 1.6. Fixed pitch rotation speed and power

The power control system accomplishes both maximum power point tracking (MPPT) and maximum power limit (MPL) functions by controlling the angle of flow of six IGBTs. The main emphasis of the thesis is placed on the problem of maximum power tracking, while power limit is discussed in Chapter 6.

Based on the momentum theory, the mechanical power absorbed by the wind turbine is

$$P_{Max} = \frac{1}{2}\rho A v^3 C_{P\_\max} \tag{1.1}$$

Where ρ is the density of air, A is the swept area, v is the wind speed and C_P is the power coefficient. From Equation 1.1, it is clear that the power captured by the

wind under a given speed is depended on the power coefficient. C_P is decided by tip speed ratio λ and blade's pitch angle β.

The tip speed ratio (TSR) is show in Equation 1.2

$$\lambda = \frac{\omega R}{v} \tag{1.2}$$

where ω is wind turbine angular velocity, R is the radius and v is the wind speed. The $C_P(\lambda, \beta)$ is a function of λ and β.

$$C_P(\lambda, \beta) = 0.5176(116\frac{1}{\lambda_i} - 0.4\beta - 5)e^{-21\frac{1}{\lambda_i}} + 0.0068\lambda \tag{1.3}$$

$$\frac{1}{\lambda_i} = \frac{1}{\lambda + 0.08\beta} - \frac{0.035}{\beta^3 + 1} \tag{1.4}$$

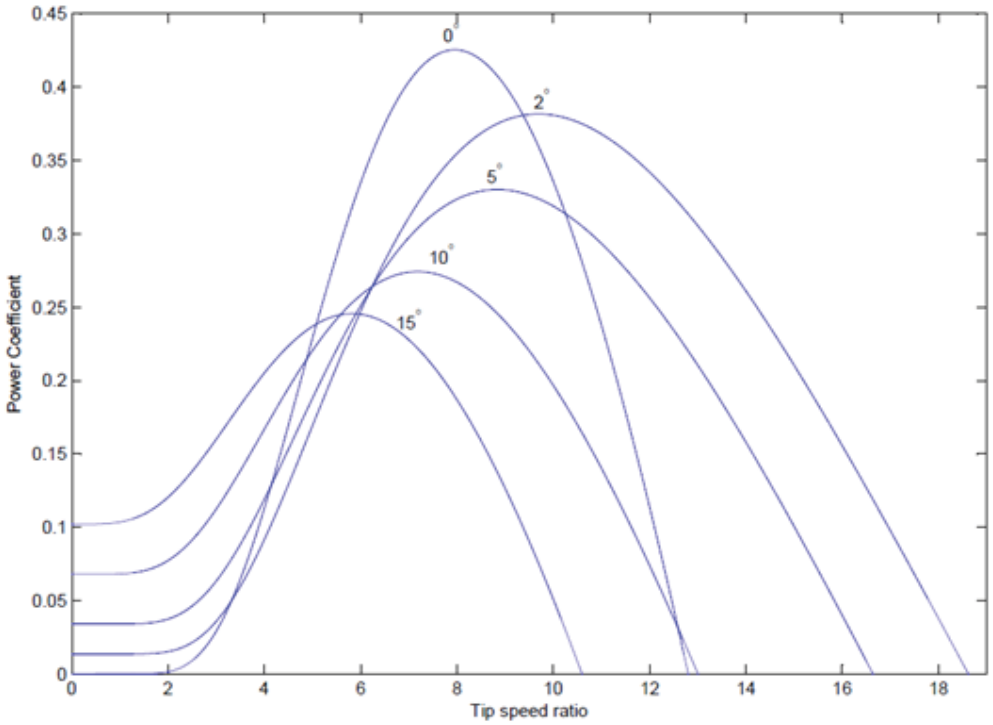

Fig. 1.7. Power coefficient VS TSR

As shown in Fig 1.7, for fix pitch angle, the power coefficient is decided by wind speed and generator rotation speed. There is only one rotation speed that makes the

power system output the maximum power under a certain wind speed [15]. Assuming the wind turbine operates smoothly on the A point of P_{opt} curve under a wind speed v_3 at the very beginning. Then the output power of wind turbine is equal to the mechanical input power of the generator which is P_a in Fig 1.8. At this time, the wind machine rotates at the speed ω_1. Then, at a certain time, the wind speed shifts instantly from v_2 to v_1. Corresponding, the operation point switches from A to B and the output power suddenly changes from P_a to P_b while the rotation speed keeps ω_1 at the transient point. Due to inertia effect and lagging of regulating process, the generator still works at A which would lead to the input power higher than the output power. The out of balance between input and output power will cause acceleration of the rotation speed. In the acceleration process, the wind turbine increase speed with the curve B to C and the generator increase speed with the curve A to C. When the wind turbine power curve intersect the optimal operation curve at C, the input and output power reach balance again with the rotation speed ω_2. ω_2 is the relative optimal rotation speed under wind speed v_2. The deceleration process from v_1 to v_2 could be analysis in the same way.

1.3.3 Maximum Power Point Tracking Algorithm Review

The former research is focused on three type of maximum power method which is TSR control, power signal feedback (PSF) control and Hill climbing method.

TSR control use wind turbine rotor speed to maintain an optimal TSR. Both the wind speed and turbine speed need to be measured for TSR calculation, and the optimal TSR must be given to the controller. The first barrier to implement TSR control is the wind speed measurement, which adds to system cost and presents difficulties in practical implementations. The second barrier is the need to obtain the optimal value of TSR, which is different from one system to another. This dependency on turbine-generator characteristics results in custom-designed control software tailored for individual wind turbines.

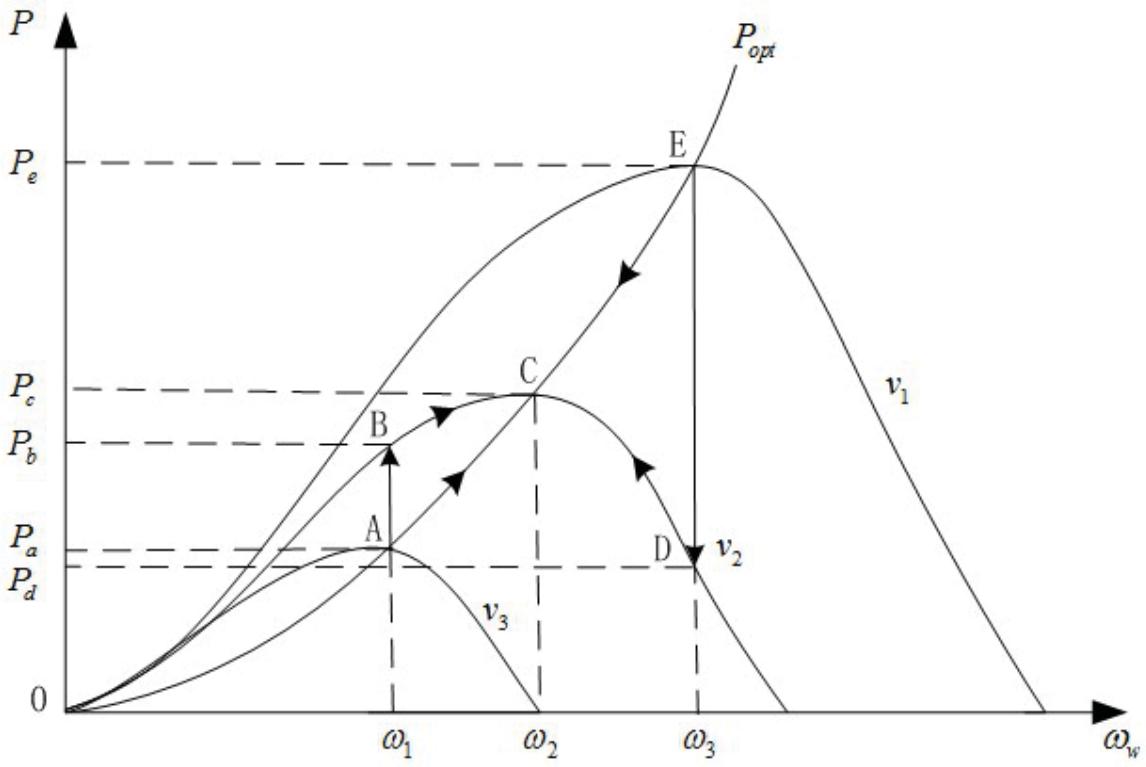

Fig. 1.8. Maximum power point tracking principle

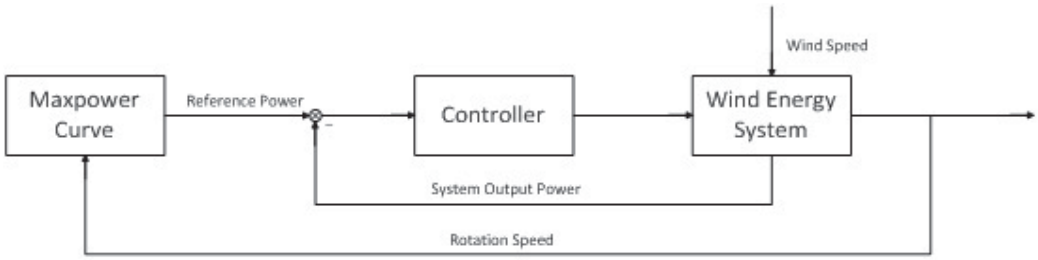

Fig. 1.9. PSF control

PSF control requires the knowledge of the wind turbine's maximum power curve and tracking of this curve through its control mechanisms. This maximum power

curve needs to be obtained via simulations or tests for individual wind turbines, which makes PSF control difficult and expensive to implement in practice.

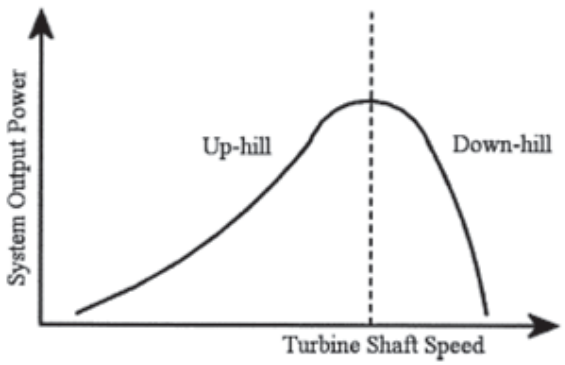

Fig. 1.10. Hill climbing control

To overcome the aforementioned drawbacks, HCS control has been proposed to continuously search for the peak output power of the wind turbine. HCS control works well only when the wind turbine inertia is very small so that the turbine speed reacts to wind speed almost instantaneously. For large inertia wind turbines, the system output power is interlaced with the turbine mechanical power and rate of change in the mechanically stored energy, which often renders the HCS method ineffective.

Equation 1.5 describes the relationship between the turbine mechanical power P_m, and the electrical system output power P_{out}, where is the load of the turbine; is the friction torque, is the turbine's angular speed, J is the turbine's moment of inertia, and is the overall electrical efficiency of the system from generator input to inverter output. When J is very small, HCS control can search for a maximum through regulations. When J is not negligible, HCS control fails to reach the maximum power points under fast wind variations, thus severely limiting the usefulness of this method for large wind turbines.

$$P_m = P_{load} + T_f * \omega + \omega * J\frac{d\omega}{dt} = \frac{1}{\eta}P_{out} + T_f * \omega + \omega * J\frac{d\omega}{dt} \tag{1.5}$$

It is thus highly desirable to develop a maximum power extraction method for wind turbines, which does not require the measurement of wind speed or turbine rotor speed, is independent of system characteristics, and is applicable to large and small wind turbines. The authors in [16] [17]have developed a new intelligent maximum wind power extraction algorithm which meets these criteria.

1.4 Main Contributions

Compared with MW-sized big wind power, the energy utilization ration of KW-sized small wind power is lower which makes it less competitive. To improve the performance, many techniques are applied. This work focuses on maximum power point tracking on variable speed wind turbine. Based on a 5 KW permanent magnet synchronous generator, a simulation model is developed. Rotor flux oriented vector control is used to form the generator side energy tracking system. Speed sensorless algorithm is put into use to remove the speed sensors so that the cost would be reduced and the reliability could be guaranteed. By using this algorithm, both rotation speed and the position angle are available. In TSR power tracking method, it is hard to get the accurate value of coefficient K. In order alleviate the disadvantage, hill climbing method is chosen to replace the TSR control. Based on the data collected by using hill climbing method, a fuzzy control box is designed to optimize the performance.

1.5 Thesis Overview

In Chapter 2, a Matlab simulation model of permanent magnet synchronous generator is built using field-oriented vector control. Power control closed-loop and current control closed-loop are designed. Using the vector control, d-axis and q-axis voltage decoupling is made for PWM signals create. Model is run to test both the dynamic characteristic and steady state characteristic. In Chapter 3, the TSR method is first applied on the model. Directly measuring the wind machine rotation speed, extra tachometer is required. In order to get rid of the device, an EFM control is attempted

as the second control method.As the accurate coefficient is hard to achieve, a fuzzy-based hill climbing control box is designed based on the previous two methods. In Chapter 4, the simulation model is run to verify the static and dynamic characteristic results for three different control methods. Matlab design is also conclude for detail description. Chapter 5 analyzes the overall simulation results. In Chapter 6, further work and recommendations are given. Intelligent algorithm may apply to optimize the fuzzy box. Maximum power limit control could be done in the future so that a complete power control system is built.

2. MODELING

2.1 Permanent Magnet Synchronous Generator Mathematics Model

A permanent-magnet wind power system is mainly comprised of permanent-magnet synchronous generator, generator side converter, direct current capacitor and grid side converter. Among all these parts, the focal point in the thesis is the generator side converter. The generator side converter regulates the generator's active power which is quite important in maximum power point tracking. The rotor flux-oriented vector control is simple and effective for small size permanent magnet synchronous generator. In the method, d-q coordinate system spins in the synchronous speed with the q-axis leads d-axis. The stator's voltage equation can be achieved when the d-axis is set on the rotor's permanent magnet flux direction.

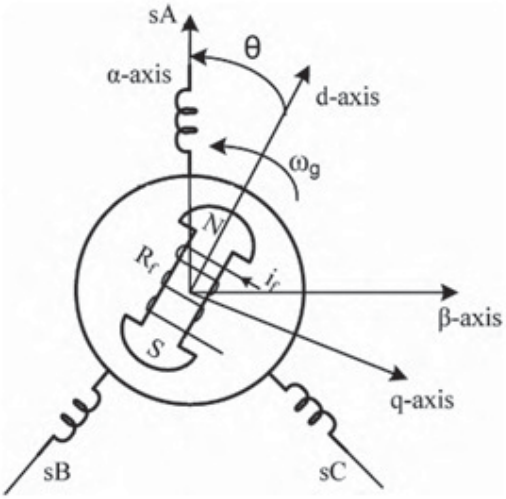

Fig. 2.1. PMSG coordinate system

In static abc coordinate system, the stator's voltage vector and the flux linkage are

$$u_s = R_s i_s + \frac{d\psi_s}{dt} + \frac{d\psi_f}{dt} \tag{2.1}$$

$$\psi_s = L_s i_s + \psi_f \tag{2.2}$$

where u_s is the generator stator voltage vector R_s is the generator's stator phase resistance i_s is the generator stator current vector ψ_s is the stator's flux linkage ψ_f is the rotor's permanent magnet flux linkage L_s is the generator's stator synchronous inductance

In rotor flux-oriented vector control, the ac permanent magnet synchronous motor stator's voltage, current and flux linkage are decomposed in to permanent magnet base wave excitation axis direction (d-axis) and rotor rotating direction advance 90 degrees direction (q-axis). The d-q coordinate system rotates at a synchronous speed ω_r as the rotor.

Then the field-oriented stator's voltage equation is

$$u_{sd} = R_s i_{sd} + \frac{d\psi_{sd}}{dt} - \omega_r \Psi_{sq} \tag{2.3}$$

$$u_{sq} = \mathrm{R_s i_{sq}} + \frac{\mathrm{d}\psi_{\mathrm{sq}}}{\mathrm{dt}} + \omega_{\mathrm{r}} \Psi_{\mathrm{sd}} \tag{2.4}$$

where ψ_{sd} is the stator's d-axis flux linkage component, Ψ_{sq} is the stator's q-axis flux linkage component, u_{sd} is the generator's stator d-axis voltage component, u_{sq} is the generator's stator q-axis voltage component, i_{sd} is the generator's stator d-axis current component, i_{sq} is the generator's stator q-axis current component.

The d-q coordinate system flux linkage is given as

$$\psi_{\mathrm{sd}} = \mathrm{L_d i_{sd}} + \psi_{\mathrm{f}} \tag{2.5}$$

$$\psi_{\mathrm{sq}} = \mathrm{L_q i_{sq}} \tag{2.6}$$

For surface-mounted permanent magnet synchronous generator, the air gap can be approximated as even. Then

$$\mathrm{L_d} = \mathrm{L_q} = \mathrm{L_s} \tag{2.7}$$

Combining Equations 2.1,2.2,2.3,2.4,2.5,2.6 and 2.7, we obtain

$$u_{\mathrm{sd}} = \mathrm{R_s i_{sd}} + \mathrm{L_s}\frac{\mathrm{di_{sd}}}{\mathrm{d_t}} - \omega_{\mathrm{r}}\mathrm{L_s i_{sq}} \tag{2.8}$$

$$u_{sq} = \mathrm{R_s i_{sq}} + \mathrm{L_s}\frac{\mathrm{di_{sq}}}{\mathrm{d_t}} + \omega_{\mathrm{r}}\mathrm{L_s i_{sd}} + \omega_{\mathrm{s}}\psi_{\mathrm{f}} \tag{2.9}$$

From Equations 2.8 and 2.9, it is shown that the stator's d-axis and q-axis current is not only affected by control voltage u_{sd} and u_{sq} but also has relationship with coupling voltage $-\omega_{\mathrm{r}}\mathrm{L_s i_{sq}}$, $\omega_{\mathrm{r}}\mathrm{L_s i_{sd}}$ and $\omega_{\mathrm{s}}\psi_{\mathrm{f}}$. The coupling voltage is the function of rotation speed ω_{r}, and it will substantially increased when the generator operates at high speed. Under this condition, the coupling voltage component will affect the output of torque current so that the output torque would be inaccurate. As a result, decouple is needed for u_{sd} and u_{sq} [11].

Using rotor flux orientation vector control method, $\mathrm{i_{sd}} = 0$, when the generator is in steady operation. Then the generator's electromagnetic torque is

$$\mathrm{T_{em}} = \mathrm{p}\psi\mathrm{i_{sq}} \tag{2.10}$$

where p is polar pair.

From Equations 2.8, 2.9 and 2.10, it is clear that the generator's electromagnetic torque is merely related with stator's q-axis current component. By adjusting the generator's electromagnetic torque, the generator's electromagnetic power and output active power could be accurately regulated. In permanent magnet synchronous generator control system there are two control loops, the outer loop and the inner loop. In outer loop or called power loop, the active power close loop PI control is used to control the set generator's stator q-axis current component. In the inner loop or called current loop, the close loop PI control works on stator's d-axis and q-axis current control [13].

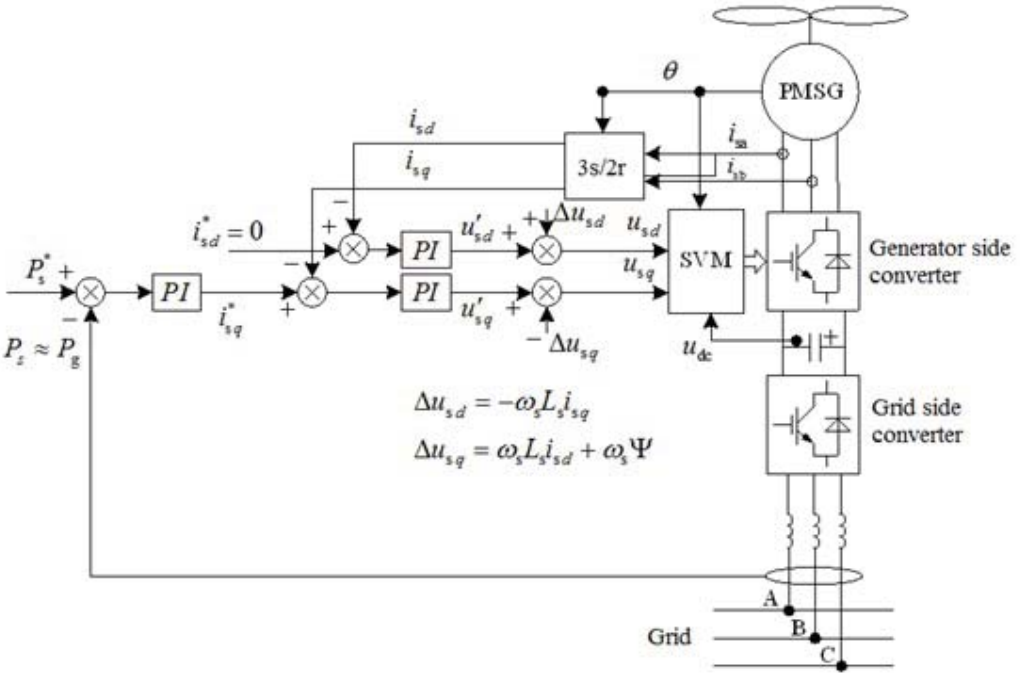

Fig. 2.2. Generator side converter control framework

2.2 Generator Side Converter Control Structure

Fig 2.2 shows the given optimal power control method framework of generator side converter power and current dual close loop. The DC side current is regulated constant by grid side converter, and it is assumed that in operation process the DC capacitor's charge-discharge power change can be ignored. If the converter cost is also neglected, then theoretically, the entire generator's output active power is feed into the grid through back to back PWM converter. So, the generator's output active power could be indirect obtained by measure the grid side feed-in active power P_g.

The active power P_s^* is used to control the generator's output active power. According to the wind machine operation characteristics in Chapter 2, the maximum power tracking control can be achieved [18] [19] [20].

2.3 Generator Side Converter Simulation

The Matlab simulation model is shown in Fig 2.2. This project focus on the research of PMSG power tracking method, the gird and the grid side converter are not taken into consideration. The dc capacitance is substituted by a 450 V DC power source for experimental simplify. The universal bridge is chosen as "IGBT/Diode".

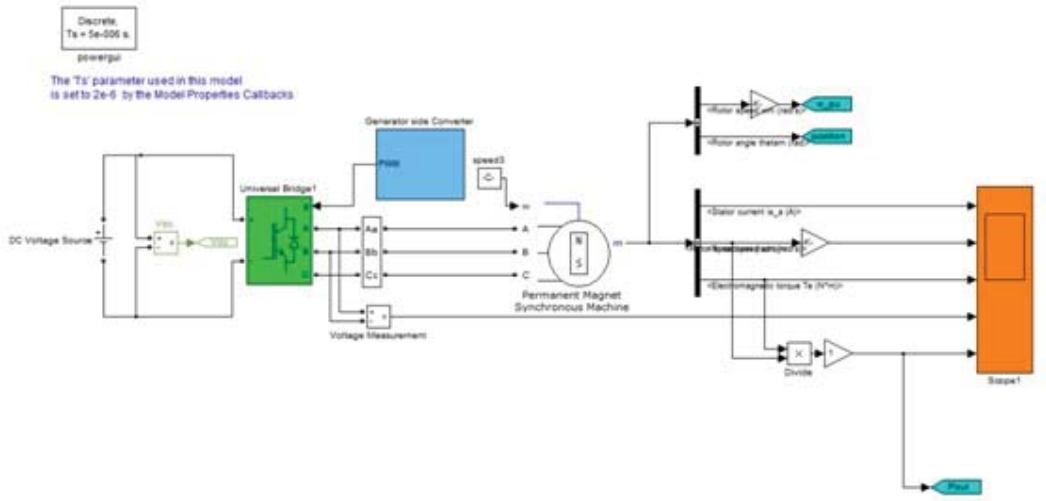

Fig. 2.3. Matlab simulation model

In this simulation model, the generator operates under a constant rotation speed. Using "Bus selector", signals such as rotor speed, stator current, rotor angle and electromagnetic torque are available. These signals are used to calculate the IGBT's fire angles of back to back PWM converter so that the dc capacitance voltage could hold as 450 V.

In Matlab, permanent magnet synchronous machine block I choose the stator phase resistance is 1.5 Ω. The d-axis inductance is 9.3 mH and the q-axis inductance is 10 mh. The permanent magnet flux linkage is 0.555 V.s. These coefficients are used for u_{sd} and u_{sq} decoupling in the current regulator block. As a multi-pole generator, the pole pair is 8 so that the high power output would be possibly available under low rotation speed.

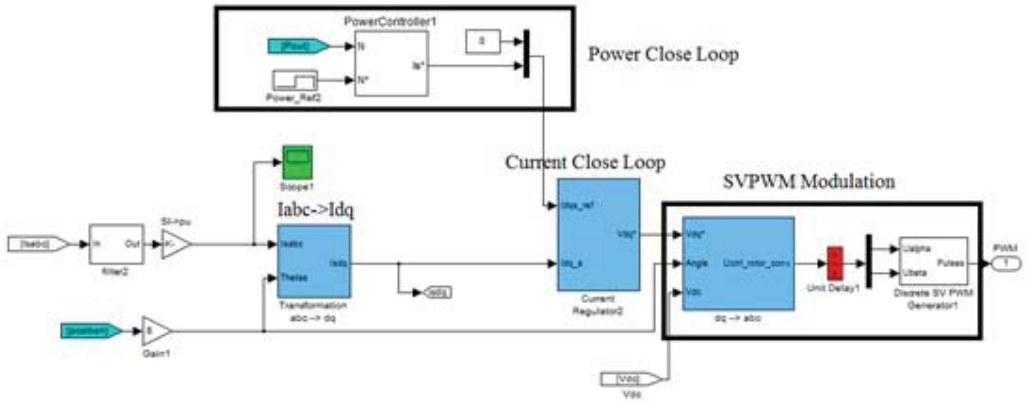

Fig. 2.4. Generator side converter

In generator side converter, the stator current is first transformed from abc coordinate system into dq coordinate system. The function of power close loop is to decide the reference current with the i_{sd} is equal to zero. Then in the current close loop (or called current regulator) the d-q axis stator current is control to follow the reference value, and decoupling components are separately added for voltage calculation on d-q axis.

2.4 Simulation Results

In simulation, the rotation speed is set constant 460 rpm which is the rated speed. And the maximum given active power is 5kw which is the rated power.

2.4.1 Static Characteristic

The simulation result shows that the wind energy system operates steadily with the 5kw reference power input. The total harmonic distortion (THD) is 0.9% that is far less than 2%. It is clear that the system has acceptable static characteristic.

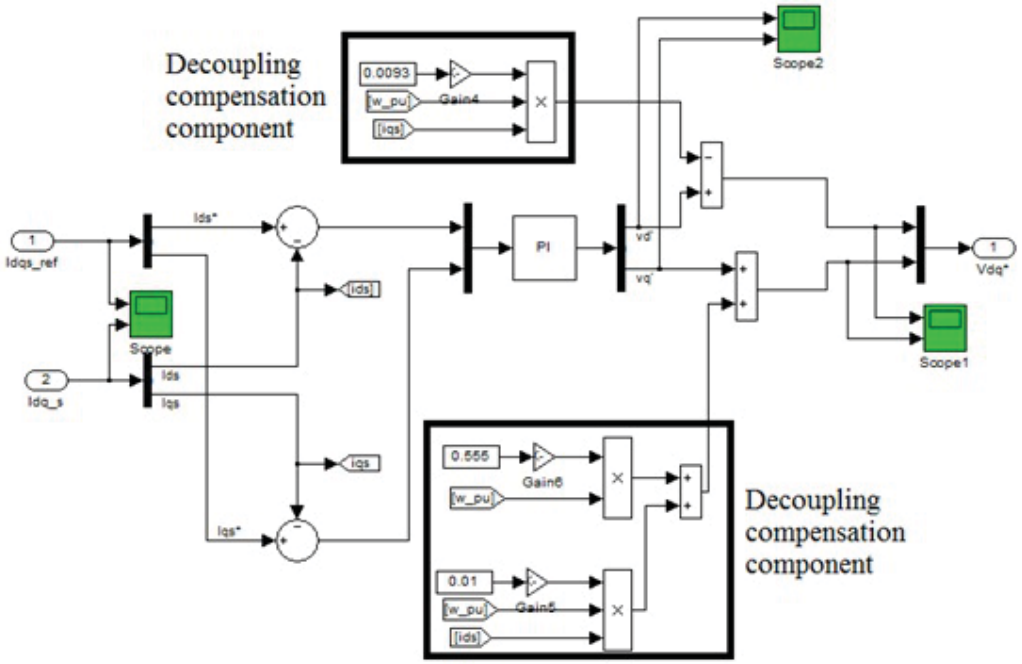

Fig. 2.5. Current regulator

2.4.2 Dynamic Characteristic

In dynamic characteristic test, the input power varies from 5kw to 1kw, then back to 5kw to under a constant rotation speed 460rpm. The result shows the stator current,electromagnetic torque and output power follow the input change in a short period of time. So the dynamic characteristic is satisfied for further control experiment.

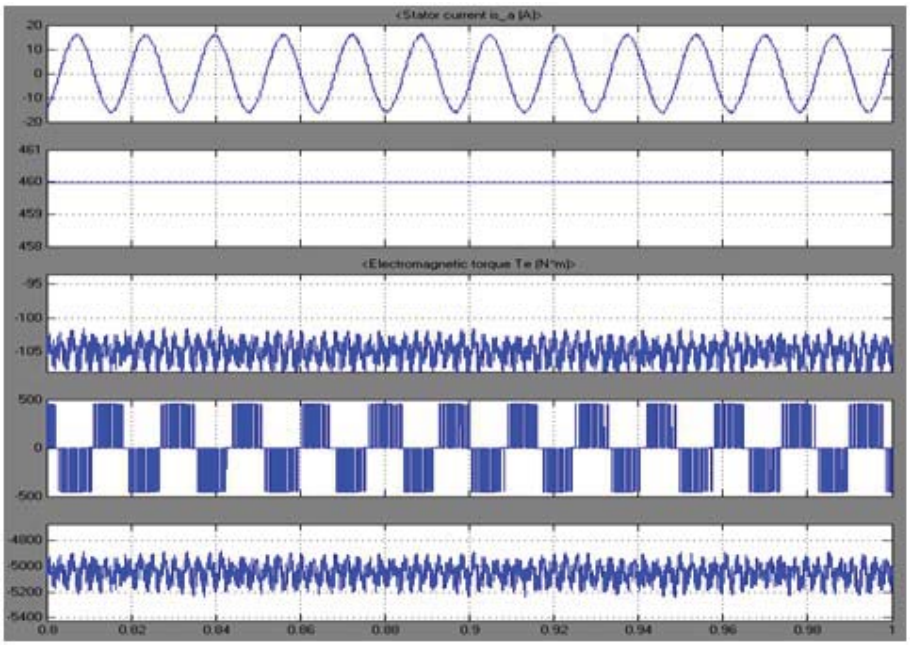

Fig. 2.6. Model static characteristic

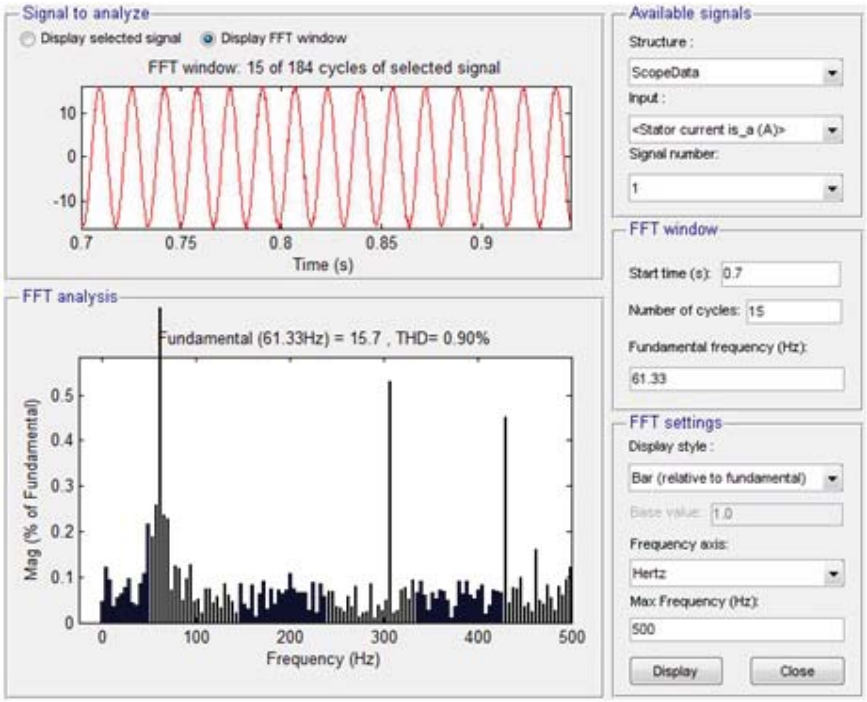

Fig. 2.7. Model stator current harmonic analysis

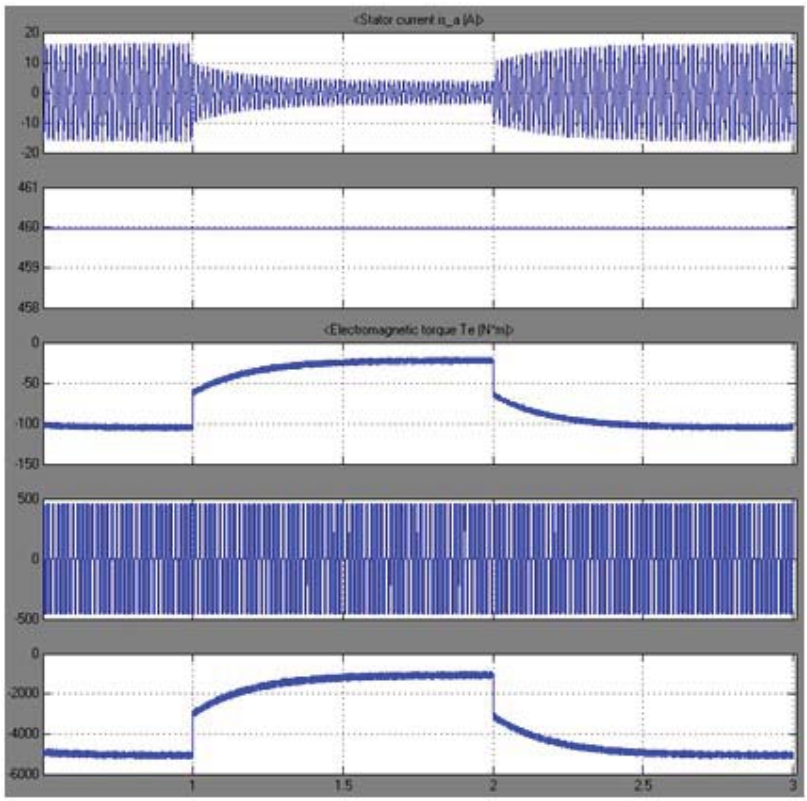

Fig. 2.8. Model dynamic characteristic

3. CONTROL METHODS FOR MAXIMUM POWER TRACKING

In this chapter, tip speed ratio control is first applied for maximum power point tracking. Then, speed sensorless algorithm is used to avoid the measurement of actual values. And TSR control is still used to test the estimate accuracy. Based on the two methods, fuzzy based hill climbing method is designed.

3.1 Tip Speed Ratio Control

3.1.1 TSR Control Method

For the knowledge of aerodynamic, the mechanical power absorbed from the wind can be written in Equation 3.1.

$$P_{Max} = \frac{1}{2}\rho A v^3 C_{P\_\max} \tag{3.1}$$

where ρ is the density of air, A is the swept area, v is the wind speed ,C_P is the power coefficient, the function of C_P is decided by tip speed ratio λ and blade's pitch angle β.

The tip speed ratio (TSR) is

$$\lambda = \frac{\omega R}{v} \tag{3.2}$$

Combine Equations 3.1 and 3.2, then the optimal power is shown below

$$P_{opt} = K_w \omega_w^3 \tag{3.3}$$

For fixed pitch wind machine used in this project, K_w is a constant value that only has relationship with wind machine characteristic [21].

In order to achieve the maximum wind power tracking, the reference active output power P_1^* is indispensability.

Equations 3.5 and 3.6 show the power relationship when wind machine operates on optimal power curve and output the maximum power.

$$P_1^* = K_w \omega_s^3 - \Delta P \tag{3.4}$$

$$\Delta P = P_{cu1} + P_{fe1} + P_f \tag{3.5}$$

P_{cu1} is the is the stator copper loss

P_{fe1} is the core loss

P_f is the aerodynamic losses

In rotor flux orientation control theory, the q-axis current component is proximately linear with the torque. As a result, P_1^*/ω_s could be used for the stator's given q-axis current reference, as shown in Fig 3.1 [22].

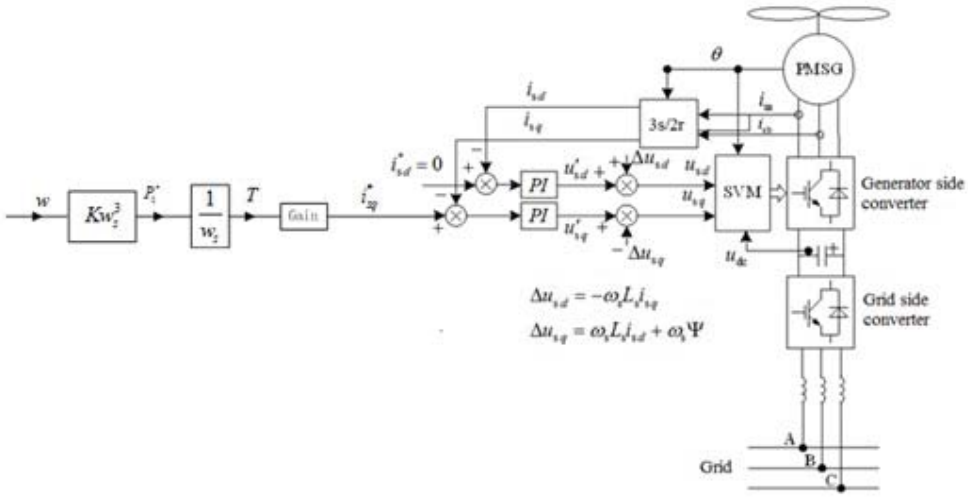

Fig. 3.1. TSR control system framework

3.1.2 System Framework of TSR Control

Since wind power system has outstanding steady-state characteristic and dynamic characteristic. It is time to add the wind machine into the system and see the power tracking.

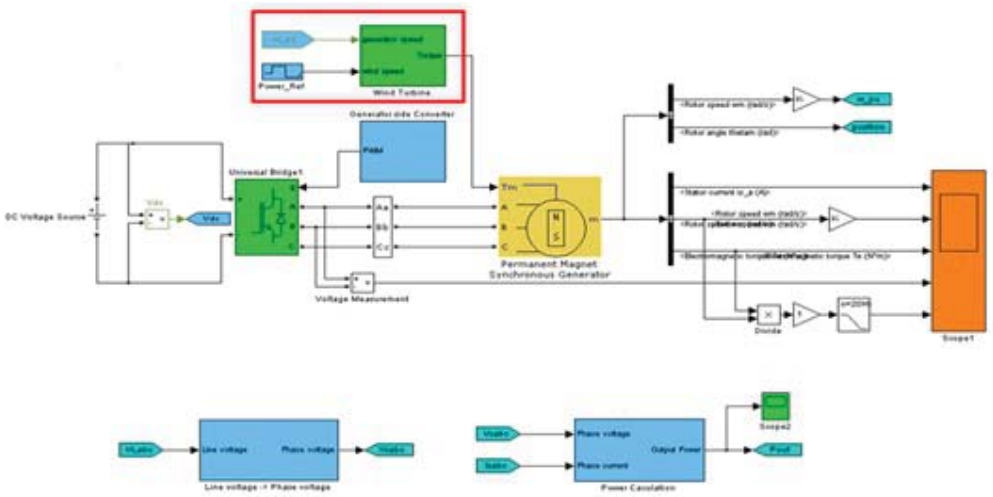

Fig. 3.2. TSR control framework

At first, the input of permanent magnet synchronous generator module is changed from power to torque. The input torque is under the control of wind turbine block with two control input generator rotation speed and wind speed.

3.1.3 TSR Power Tracking Module Design

In TSR control, the power close loop block is replaced by the maximum power tracking block.

3.2 Speed Sensorless Control

Using maximum power point tracking method, the accurate value of rotor position and rotor rotation speed is necessary for calculation. In some wind machines, mechanical sensors are used. However, the mechanical position sensors would increase the cost and reduce the reliability. The designed lifetime of a wind power system is around 15 years, while position sensor needs to be adjusted during the lifetime circle. Take into considering that the wind machine is placed on the tower which might be

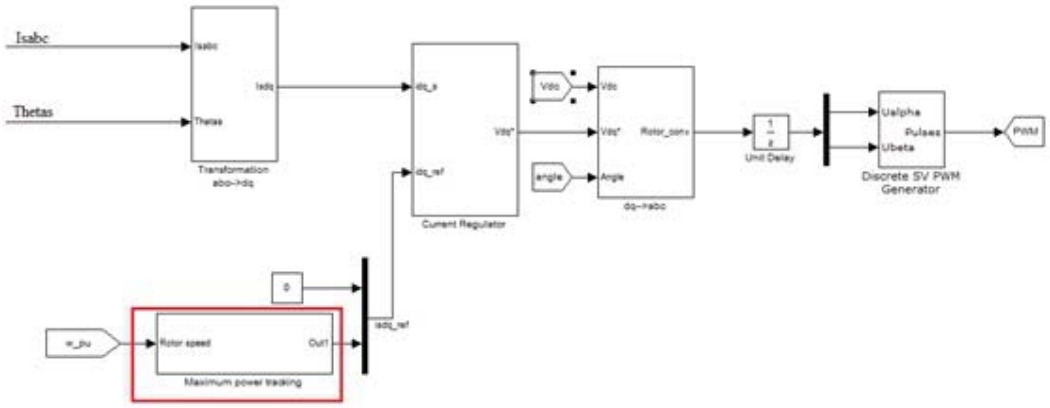

Fig. 3.3. TSR generator side converter

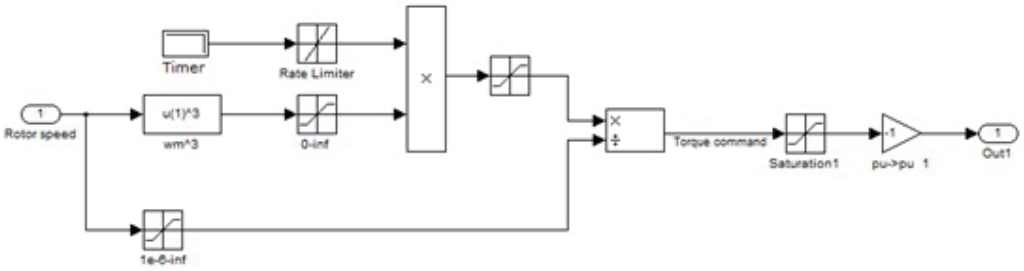

Fig. 3.4. TSR maximum power tracking

several meters high, it is quite inconvenient to use the speed-sensor in application. As a result, speed sensorless control is gradually become popular in industrial application in recent years [23] [24].

3.2.1 Speed Sensorless Control Method

In rotor flux-oriented synchronous rotation d-q coordinate system, the stator's voltage can be written as

$$\begin{bmatrix} u_d \\ u_q \end{bmatrix} = \begin{bmatrix} R + L_d p & -\omega_r L_q \\ \omega_r L_d & R + L_q p \end{bmatrix} \begin{bmatrix} i_d \\ i_q \end{bmatrix} + \omega_r \psi_f \begin{bmatrix} 0 \\ 1 \end{bmatrix} \tag{3.6}$$

where u_d,u_q is the d-q axis voltage

i_d,i_q is the d-q axis current

R is the stator winding resistance

L_d,L_q is the d-q axis induction

ω_r is the rotor rotation speed

ψ_f is the rotor permanent magnet excitation flux

p is the differential operator $\frac{d}{dt}$

In sensorless control, the rotor position $\hat{\theta}$ is gained through estimation. There is error $\Delta\theta$ between actual position θ and the estimated position $\hat{\theta}$.

Assume the actual rotor position θ is in d-q coordinate system while the estimated position $\hat{\theta}$ is in $\hat{d} - \hat{q}$ coordinate system. The two-phase stationary reference framework is $\alpha - \beta$.

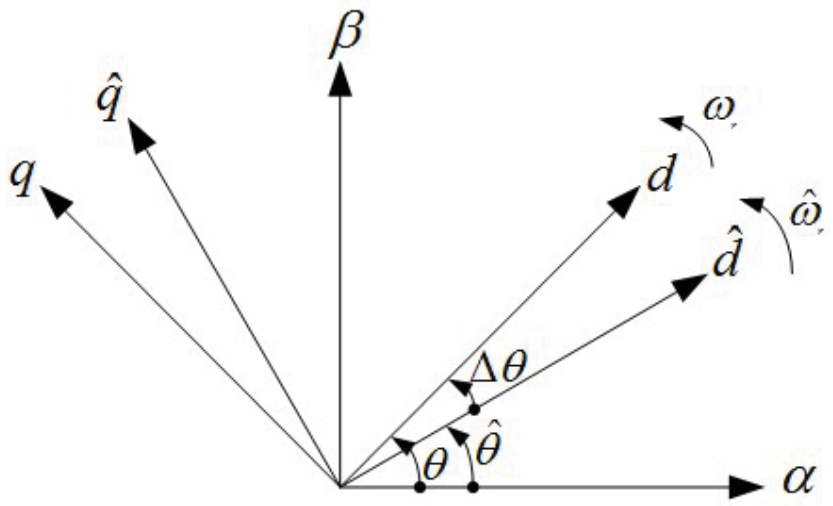

Fig. 3.5. Rotation coordinate system

then Equation 3.6 can be written as:

$$\begin{bmatrix} u_d \\ u_q \end{bmatrix} = \begin{bmatrix} R + L_d p & -\omega_r L_q \\ \omega_r L_q & R + L_d p \end{bmatrix} \begin{bmatrix} i_d \\ i_q \end{bmatrix} + \begin{bmatrix} 0 \\ \omega_r \psi_f + (L_q - L_d)\, p i_q + \omega_r (L_d - L_q) i_d \end{bmatrix} \tag{3.7}$$

Make $E = \omega_r \psi_f + (L_q - L_d)\, p i_q + \omega_r (L_d - L_q) i_d$,E is the expand back emf (EMF) then Equation 3.7 could be changed as

$$\begin{bmatrix} u_d \\ u_q \end{bmatrix} = \begin{bmatrix} R + L_d p & -\omega_r L_q \\ \omega_r L_q & R + L_d p \end{bmatrix} \begin{bmatrix} i_d \\ i_q \end{bmatrix} + E \begin{bmatrix} 0 \\ 1 \end{bmatrix} \tag{3.8}$$

According to the corresponding relations between d-q and $\hat{d} - \hat{q}$ coordinate system, the d-q axis voltage u_d and u_q can transform to the axis voltage and in $\hat{d} - \hat{q}$ coordinate system.

$$\begin{bmatrix} \hat{u}_d \\ \hat{u}_q \end{bmatrix} = \begin{bmatrix} R + L_d p & -\omega_r L_q \\ \omega_r L_d & R + L_q p \end{bmatrix} \begin{bmatrix} \hat{i}_d \\ \hat{i}_q \end{bmatrix} + \begin{bmatrix} 0 & L_d \\ -L_d & 0 \end{bmatrix} \begin{bmatrix} \hat{i}_d \\ \hat{i}_q \end{bmatrix} p\Delta\theta + E \begin{bmatrix} -sin\Delta\theta \\ cos\Delta\theta \end{bmatrix} \tag{3.9}$$

From Equation 3.9, the EMF can be written as

$$E \begin{bmatrix} -sin\Delta\theta \\ cos\Delta\theta \end{bmatrix} = \begin{bmatrix} \hat{u}_d \\ \hat{u}_q \end{bmatrix} - \begin{bmatrix} R + L_d p & -\omega_r L_q \\ \omega_r L_d & R + L_q p \end{bmatrix} \begin{bmatrix} \hat{i}_d \\ \hat{i}_q \end{bmatrix} - \begin{bmatrix} 0 & L_d \\ -L_d & 0 \end{bmatrix} \begin{bmatrix} \hat{i}_d \\ \hat{i}_q \end{bmatrix} p\Delta\theta \tag{3.10}$$

So the rotor position estimation error $\Delta\theta$ is

$$\Delta\theta = -arctan\left(\frac{\hat{u}_d - R\hat{i}_d - L_d p\hat{i}_d + \omega_r L_q \hat{i}_d - L_d \hat{i}_d p\Delta\theta}{\hat{u}_q - R\hat{i}_q - L_d p\hat{i}_q - \omega_r L_d \hat{i}_q + L_d \hat{i}_d p\Delta\theta}\right) \tag{3.11}$$

When generator operates steadily, both the voltage and current of d-q axis are constant, then pi=0. Consider the time constant of generator is big, the change of $\Delta\theta$ can be ignored, then $p\Delta\theta \approx 0$.

As a result, Equation 3.11 can be simplified as

$$\Delta\theta = -arctan(\frac{\hat{u}_d - R\hat{i}_d + \omega_r L_q \hat{i}_q}{\hat{u}_q - R\hat{i}_q - \omega_r L_q \hat{i}_d}) \tag{3.12}$$

$\Delta\theta$ can be computed through Equation 3.12, then and the rotation speed $\hat{\omega}_r$ and the rotator position $\hat{\theta}$ could be estimated. $\hat{\theta}$ is equal to θ when $\Delta\theta$ is zero [12] [25].

3.2.2 Phase Loop Locker

By calculating the rotor position error $\Delta\theta$, then it is easy to know whether $\hat{\theta}$ is leading or lagging θ. When the estimated rotor position $\hat{\theta}$ leads the actual rotor position θ, then the estimated rotation speed $\hat{\omega}_r$ should be decreased. Otherwise, the speed $\hat{\omega}_r$ should be increased. The estimated rotor position would be available when take a integration of $\hat{\omega}_r$.

Fig 3.6 shows the operation of phase loop locker control. The estimated rotor position $\hat{\theta}$ is used as feedback for synchronous rotation coordinate transformation. The calculated $\hat{d} - \hat{q}$ axis voltage $\hat{u}_d$, $\hat{u}_q$ and current $\hat{i}_d$, $\hat{i}_q$ are used to count the rotor position error $\Delta\theta$ through Equation 3.12. The output of PI regulator is estimated rotation speed $\hat{\omega}_r$. Fig 3.7 describes the flow chart of the speed sensorless control.

3.2.3 System Framework of Speed Sensorless Control

The maximum power point tracking module is the same as the one used in TSR control. The position detection module is added to calculation the estimate rotation speed and position.

In Fig 3.8, thetae is the estimated rotor position theta is the actual rotor position we is the estimated rotation speed w_pu is the actual rotation speed

As we can see from Fig 3.9, the decoupling components are using estimated rotation speed instead of actual value.

3.3 Fuzzy Based Hill Climbing Method

In Section 3.2, speed sensorless control is applied to avoid the mechanical speed sensor. The estimated rotation speed and rotor position are used in maximum power

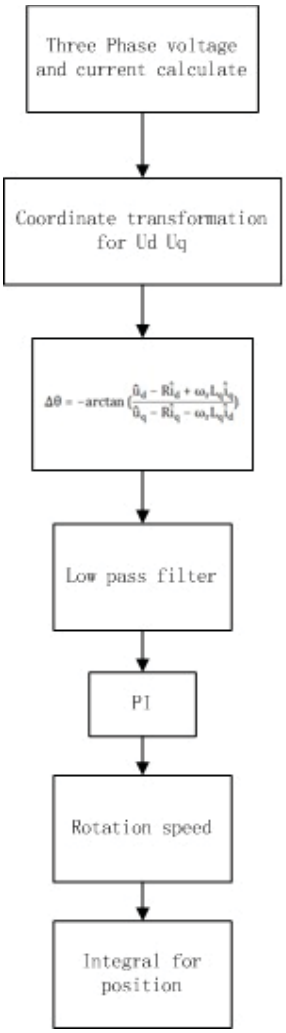

Fig. 3.6. Speed sensorless flow chart

point tracking and d-q axis voltage decoupling. The MPPT strategy $P_{opt} = K_w \omega_w^3$ is chosen to calculate the stator's q-axis reference current. However, in most of time, it is difficult to achieve the accurate value of coefficient K. Different from other control methods, Hill climb Searching (HCS) control happens to be the one that doesn't need any prior information about the turbine, pitch angle and wind characteristics.

TSR control is used to operates in start region and provides initial value for hill climbing method. Speed sensor algorithm is apply to provide estimated value

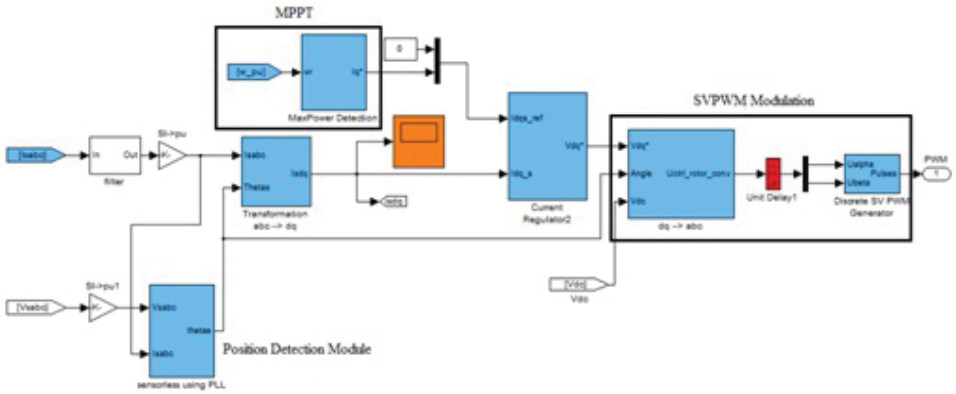

Fig. 3.7. Position detection module

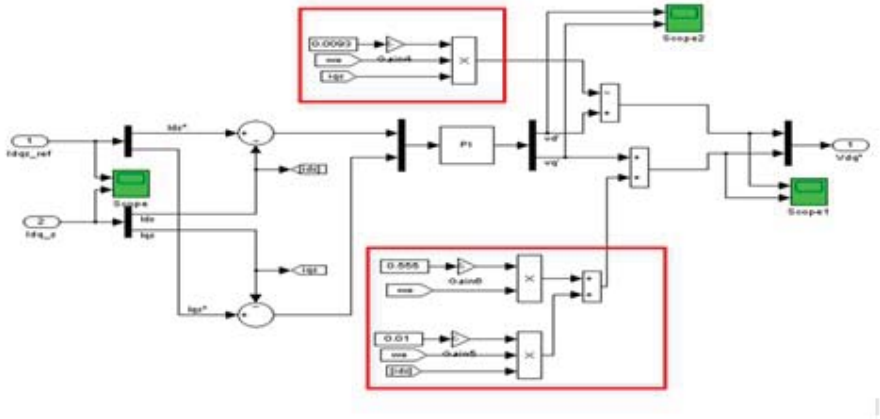

Fig. 3.8. Speed sensorless current regulator module

and replace the speed sensor. Fuzzy box replaces a lookup table and gives adaptive searching steps for the hill climbing search.

3.3.1 Hill Climbing Method

Hill climbing method is a simple method which could be written as

$$x\left(k+1\right)=x\left(k\right)+step*sign \tag{3.13}$$

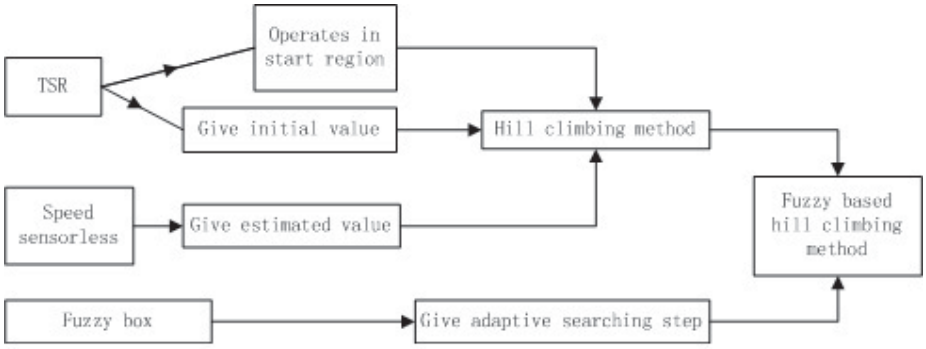

Fig. 3.9. Fuzzy based hill climb method design framework

The step is the climbing step which can be constant value or change from time to time. The sign decides whether the operation point would go up or down. q

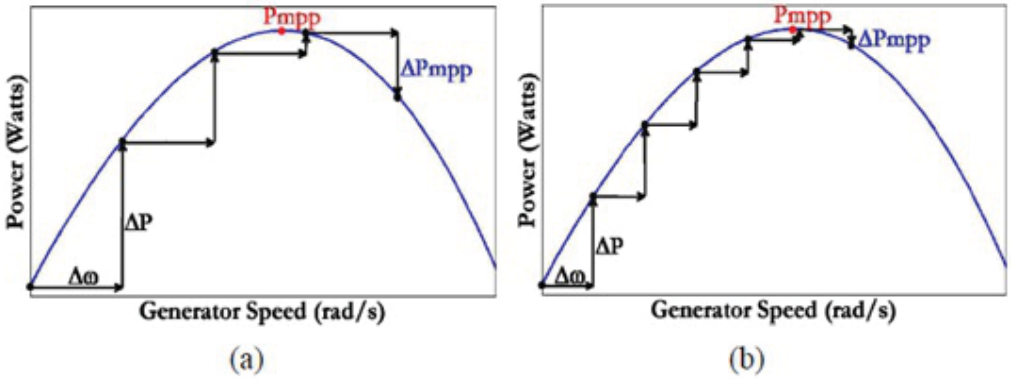

Fig. 3.10. Hill climbing method comparison

The step in Fig 3.11 (a) is larger than Fig 3.11 (b), as a result the tracking speed in 3.11 (a) is faster than in 3.11 (b). However, larger step may lead to larger oscillation and larger likelihood to pass over the maximum point. In order to achieve a tradeoff between the stability and the efficiency, the key idea in this work is to use fuzzy adaptive step size during the searching process [26].

3.3.2 System Structure of Hill Climbing Method

In this thesis, the stator q-axis current reference is chosen as the control quantity

$$iqref\,(n+1) = iqref\,(n) + M \cdot sign \cdot \left| \frac{\Delta p}{\Delta we} \right| \tag{3.14}$$

The step is decided by step coefficient M and the value of $\left|\frac{\Delta p}{\Delta we}\right|$.

Sign is decided as follows: $\Delta \mathrm{p} > 0, \Delta we > 0$ increase,sign=1, $\Delta \mathrm{p} > 0, \Delta we < 0$ keep,sign=0, $\Delta \mathrm{p} < 0, \Delta we > 0$ increase,sign=0, $\Delta \mathrm{p} < 0, \Delta we < 0$ increase,sign=1.

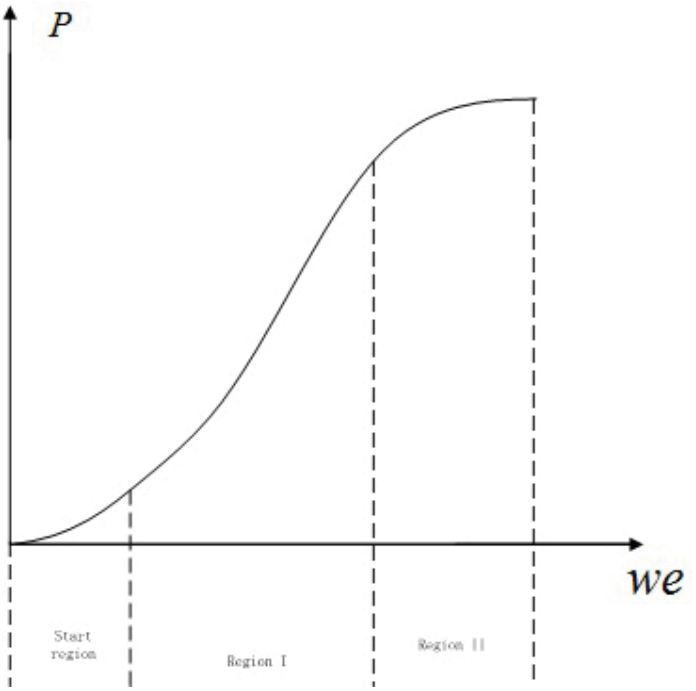

Fig. 3.11. Hill climbing method region define

As shown in Fig 3.12, Δp and Δwe is almost linear in the fast ascend region, which is region I in the figure. This simplification makes it convenient for fuzzy rule design. However, in region II the relation of Δp and Δwe is nonlinear, smaller search steps are applied for peak searching. Also, the results of $\left|\frac{\Delta p}{\Delta we}\right|$ can be used to predict the operation position point.

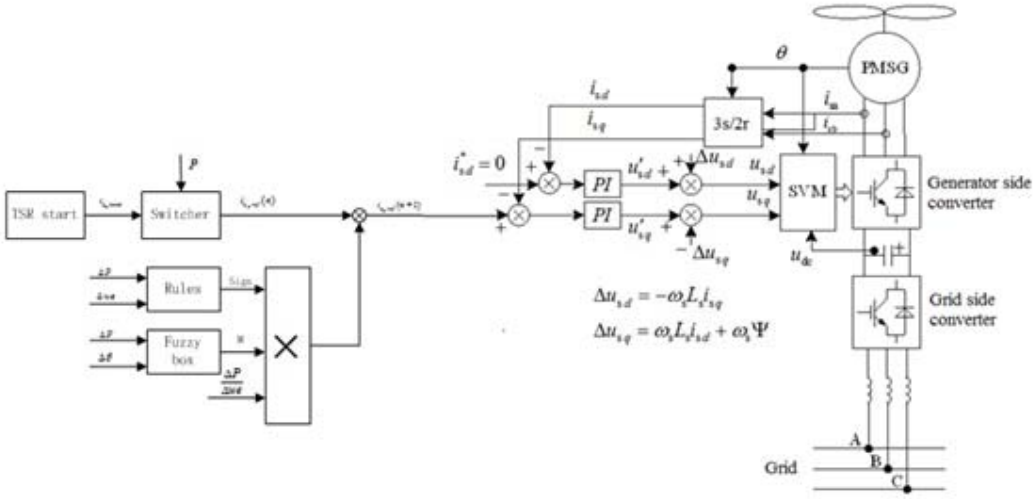

Fig. 3.12. Fuzzy control system structure

As shown in Fig 3.13. The actual rotation speed is almost the same as estimated one. The actual position is exactly the same as the estimated position.

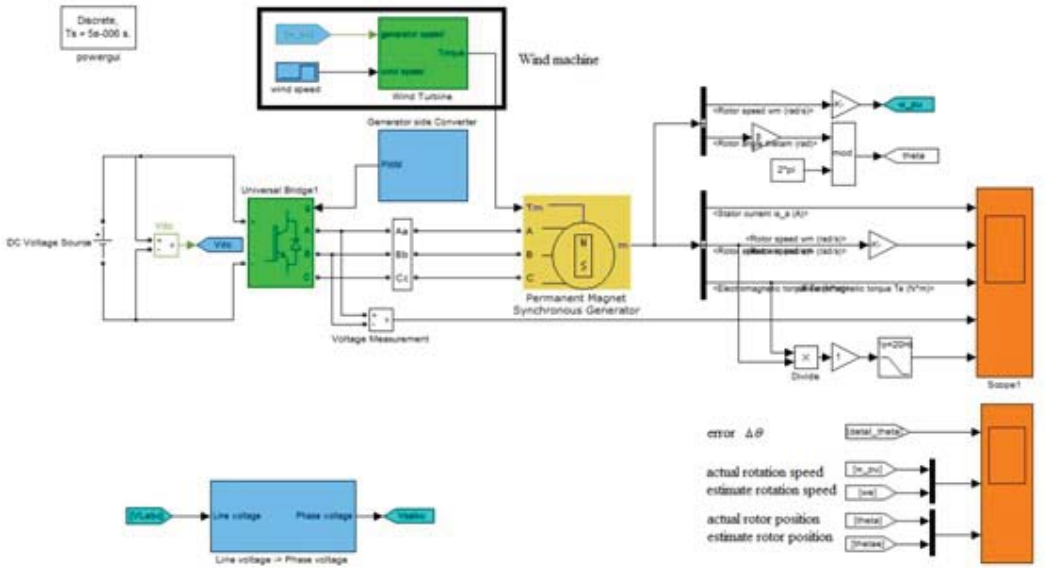

Fig. 3.13. HCM system framework

As shown in Fig 3.14, the Equation $P_{opt} = K_w \omega_w^3$ is no longer used for maximum power point tracking. Instead, the i_{s_ref} is decided be several function module.

Fig 3.15 to Fig 3.18 describe the detail of Matlab simulation model of the fuzzy based hill climbing method.

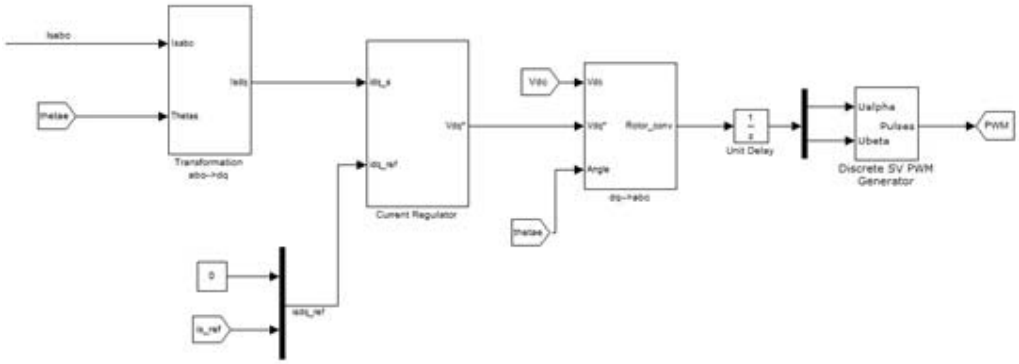

Fig. 3.14. HCM generator side converter

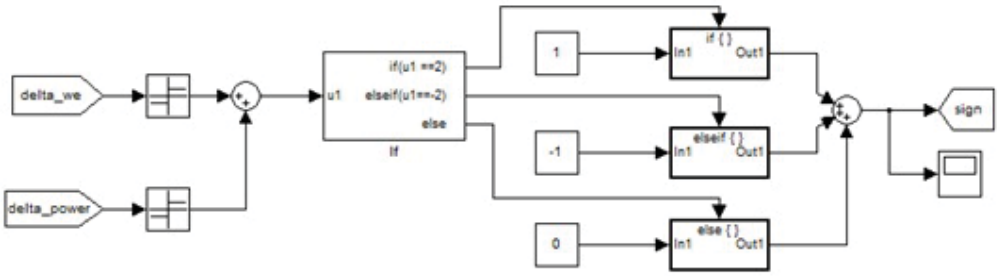

Fig. 3.15. Sign module framework

$P_{opt} = K_w \omega_w^3$ is used when power is under 300 W to start the wind machine from quiescent condition. In this case, coefficient does not need to be accurate. When the output power reaches 300 W, the controller switches to maximum power tracking operation.

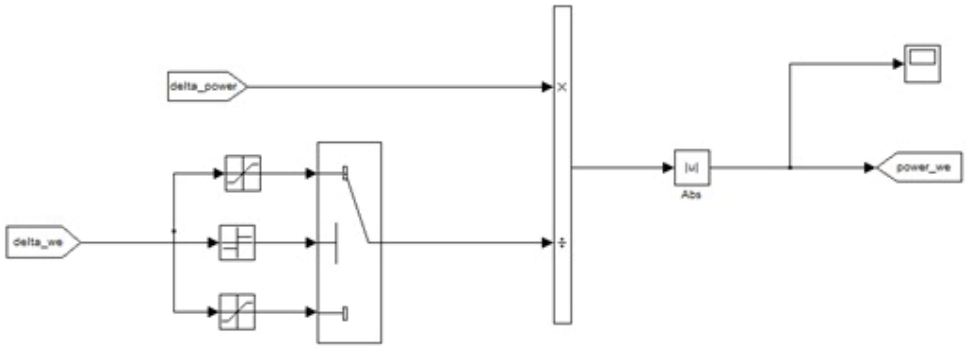

Fig. 3.16. Calculate gradient

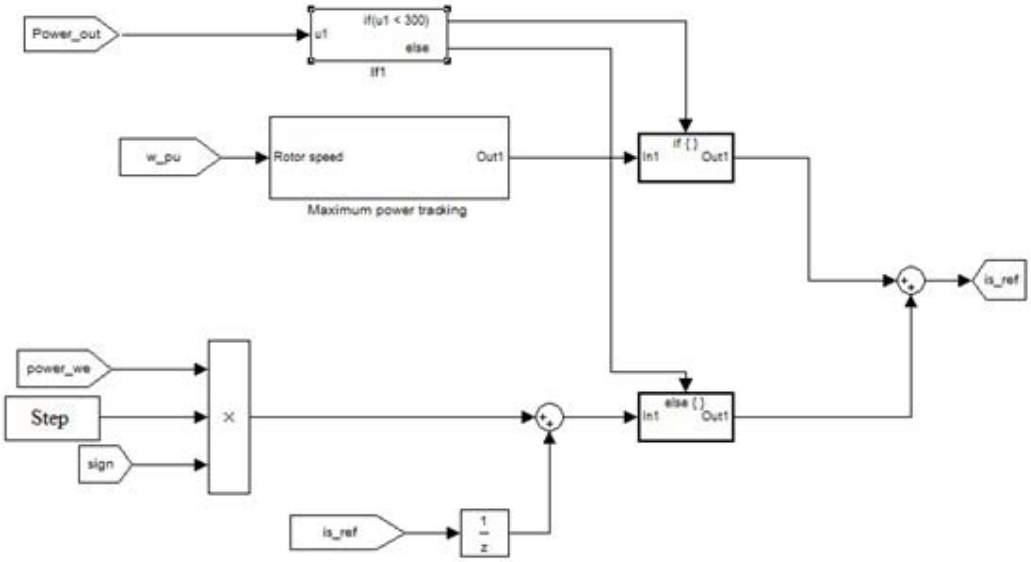

Fig. 3.17. Calculation current

3.3.3 Fuzzy Adaptive Step Design

At first, fixed step is tried in the step block to find the available range. Then a fuzzy box is designed to vary the step under proper conditions.

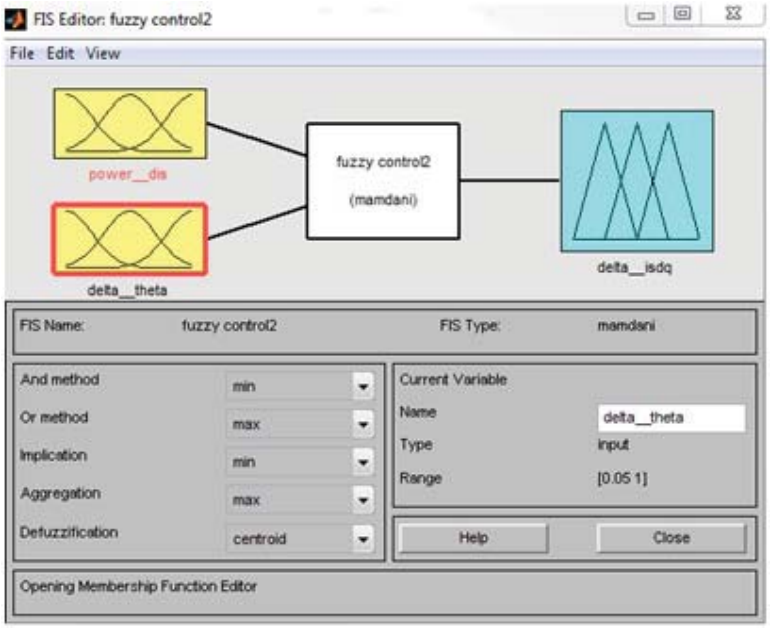

Fig. 3.18. Fuzzy control structure

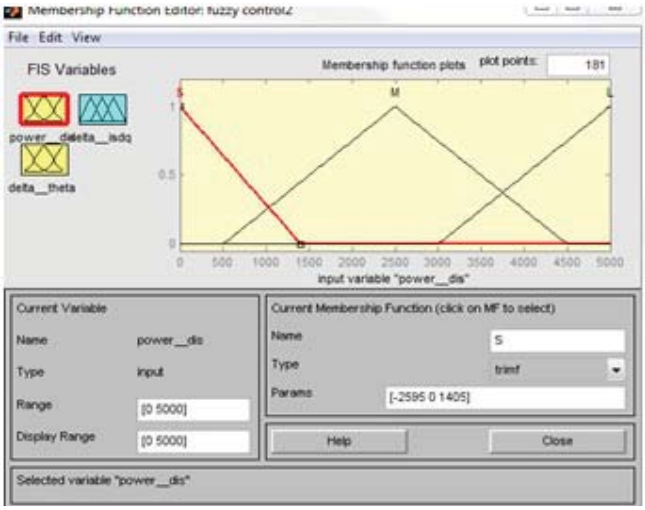

Fig. 3.19. Power membership function

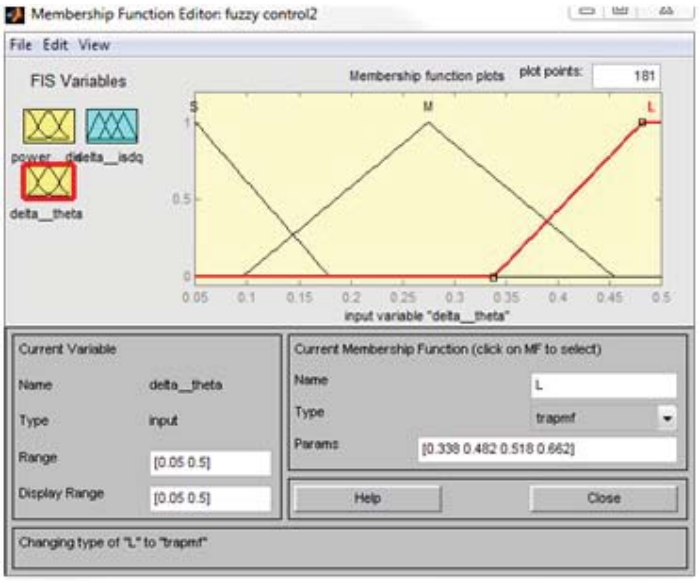

Fig. 3.20. Theta membership function

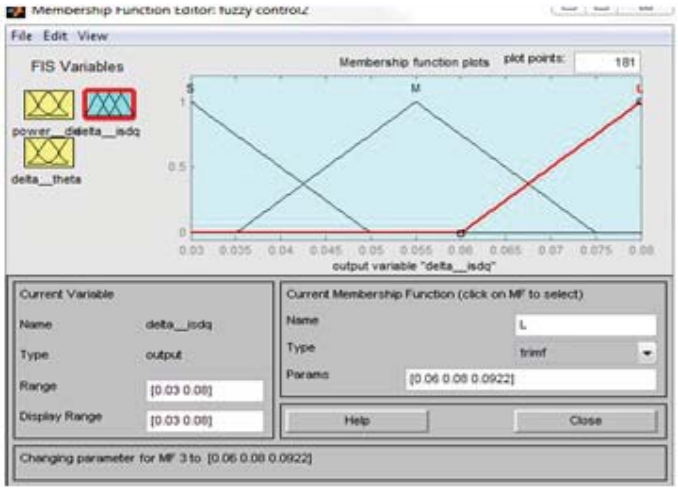

Fig. 3.21. Current membership function

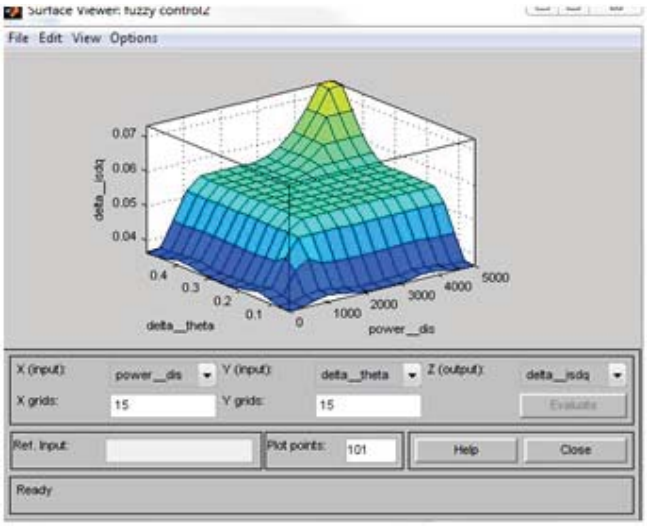

Fig. 3.22. Surface of rules

4. SIMULATION RESULTS

4.1 Wind Turbine Parameter

In the simulation, the generator base power is set to be 5 KW and the base wind speed is set to be 12 m/s.

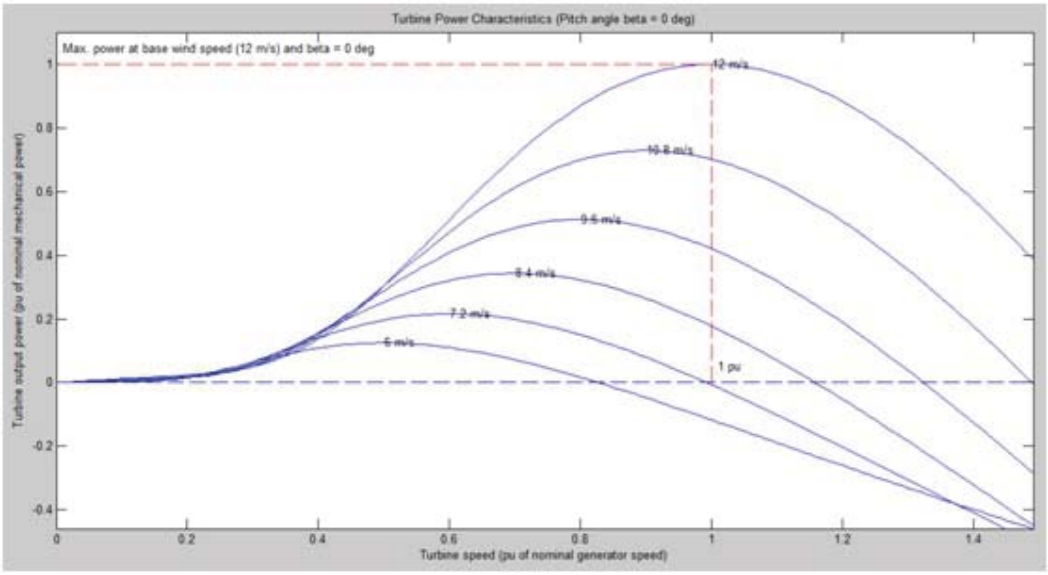

Fig. 4.1. The turbine power characteristic

As shown in Fig 4.1, the transmission rate between the wind turbine and the generator is set to be 100%.

The wind machine block in Fig 4.2 has three inputs, generator speed, pitch angle and wind speed. The generator speed is set equal to rotor speed. The pitch angle is set 0 for simplify. The rate limit is set 20 to violate sudden change.

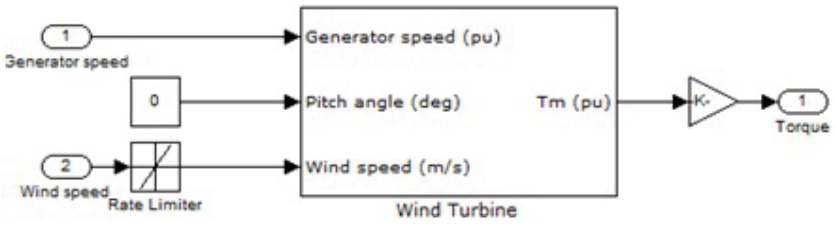

Fig. 4.2. Wind turbine module

With the consideration of $V_a + V_b + V_c = 0$, a module is design to transfer three-phase line to line voltage to three-phase line to neutral voltage, as shown in Fig 4.3.

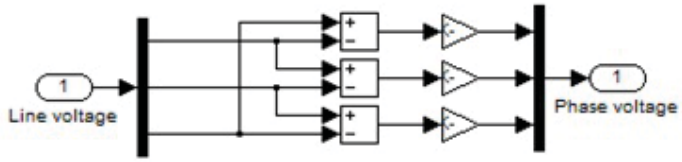

Fig. 4.3. Three phase line voltage to phase voltage

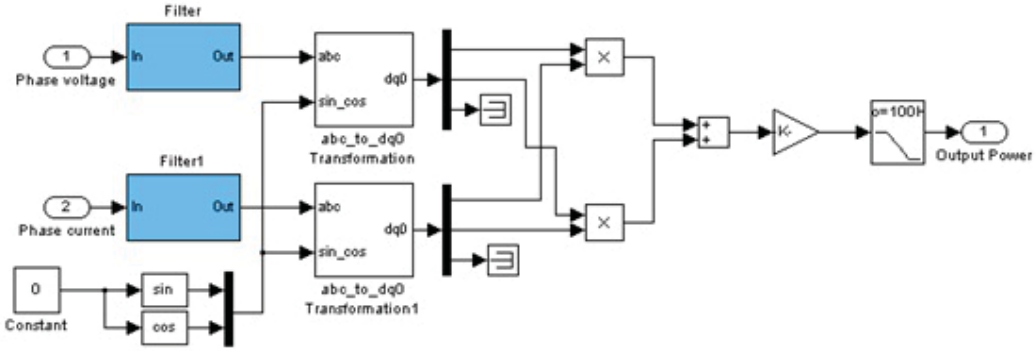

Fig. 4.4. Output power calculation block

As shown in Fig 4.4, the power calculation module uses the phase voltage and phase current to calculate the output power.

$$P_{out} = U_\alpha i_\alpha + U_\beta I_\beta \tag{4.1}$$

4.2 TSR Control Simulation

4.2.1 Static Characteristic of TSR Control

When the wind speed is 12m/s (rated power), the simulation result figure is below. The wind power system operates steadily at 5 KW output.

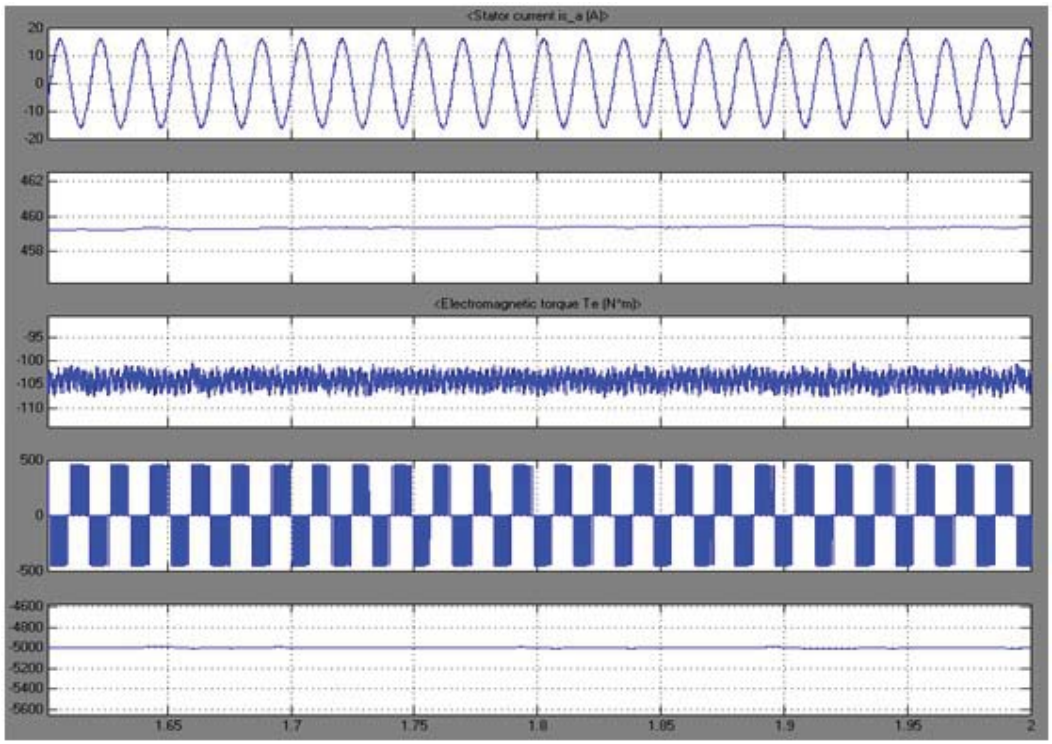

Fig. 4.5. Static characteristic of TSR control

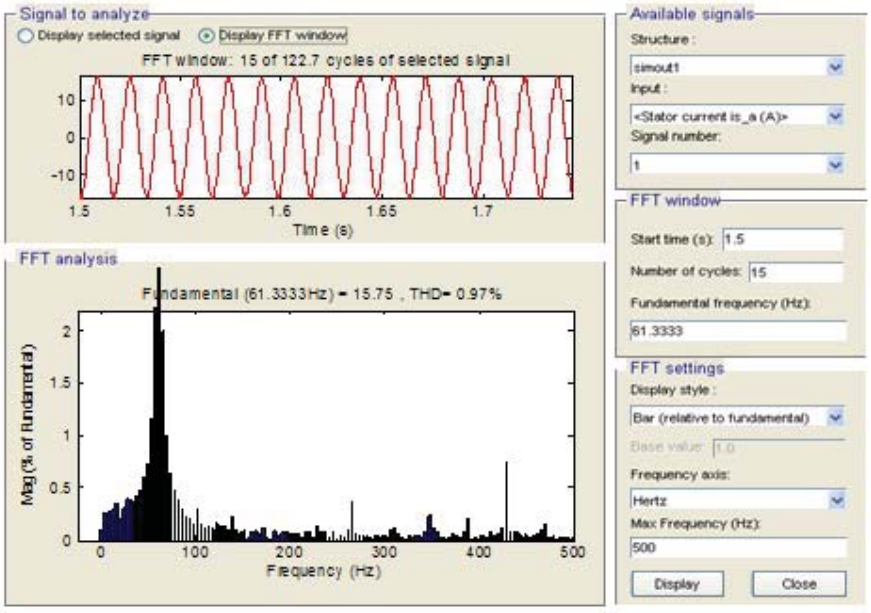

Fig. 4.6. Stator current harmonic analysis

4.2.2 Dynamic Characteristic of TSR Control

In dynamic characteristic test, the input wind speed increases from 0 to 4,8, then to 12 m/s which is the rated power.

As we can see from Fig 4.7, the stator current keeps increasing while the wind speed goes up to 12 m/s and the rotation speed finally stops at the 460 rpm. With little overshooting, the power ascend to 5000 W which is the rated power.

The test results show the stator current, electromagnetic torque and output power follow the input change in a short period of time. So the dynamic characteristic proves that the TSR control is successful applied on the previous simulation model.

4.3 Speed Sensorless Control Simulation

4.3.1 Static Characteristic of Speed Sensorless Control

The wind speed input keeps 12 m/s, the simulation result is shown in Fig 4.8.

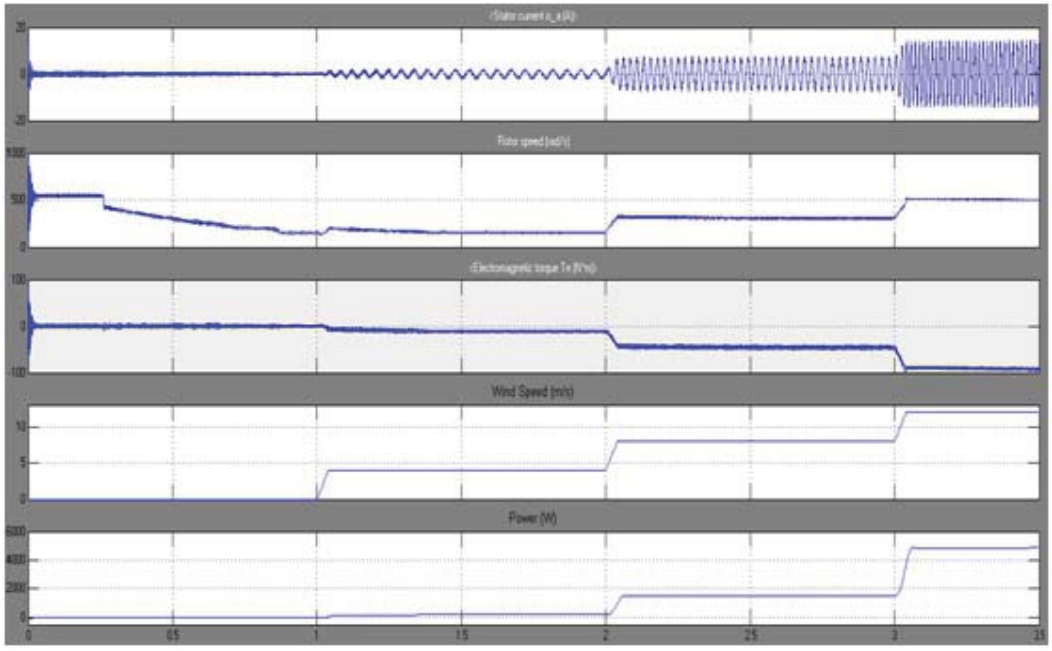

Fig. 4.7. Dynamic characteristic of TSR control

In Fig 4.9, the power system operates steadily at 5 KW. The estimation of rotation speed and rotor position is accurate.

As shown in Fig 4.9.The actual rotation speed is straight while the estimated one has small disturbance. The actual position is exactly the same as the estimated position.

4.3.2 Dynamic Characteristic of Speed Sensorless Control

The given wind speed is 9 m/s at the time 0-5 s, when t = 1.5s, the wind speed suddenly jumps to 12 m/s, then at time 2.5 m/s, the wind speed goes back to 9 m/s. The result is shown in Fig 4.10.

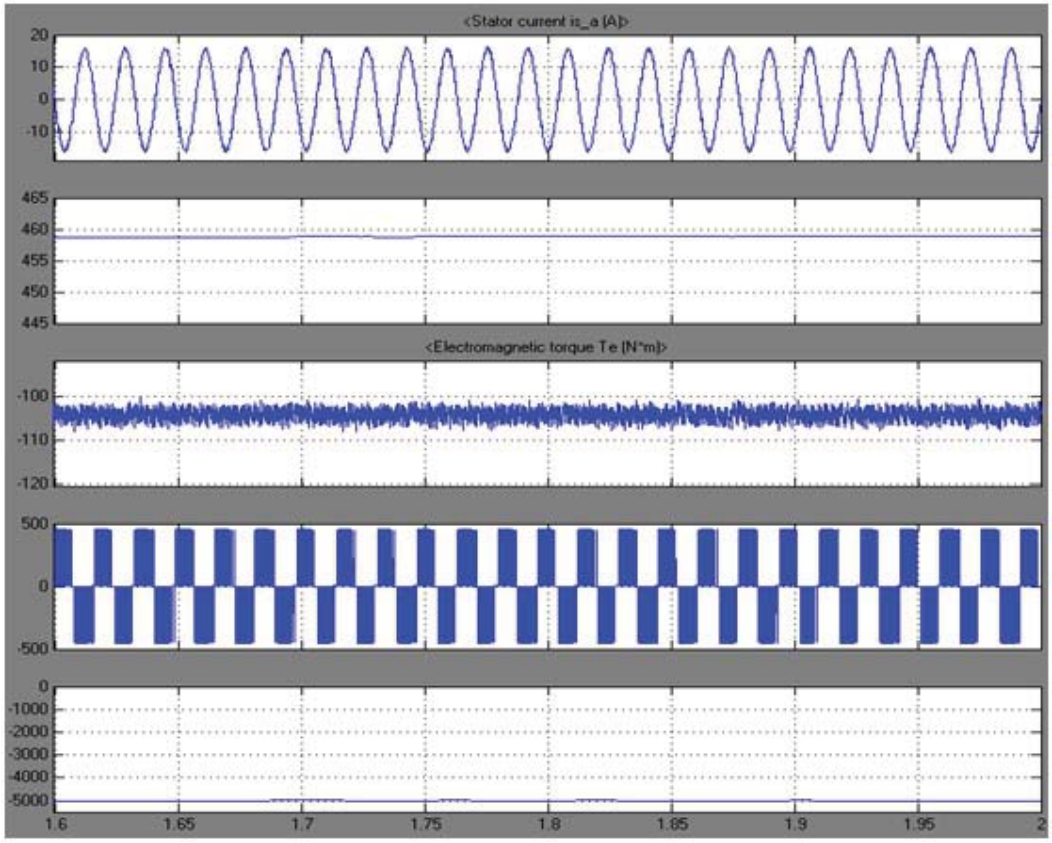

Fig. 4.8. Static characteristic of speed sensorless control

4.4 Fuzzy Based Hill Climbing Control Simulation

Wind speed acculturates from 8 m/s to the rated speed 12 m/s. From 0s to 0.5 s, the wind speed is 8 m/s. Then at 0.5 s the wind speed increases to 9 m/s until 1 s.From 1 s to 2 s is 10 m/s,and from 2 s to 3 s is 11 m/s. At 3 s the wind speed changes to 12m/s.

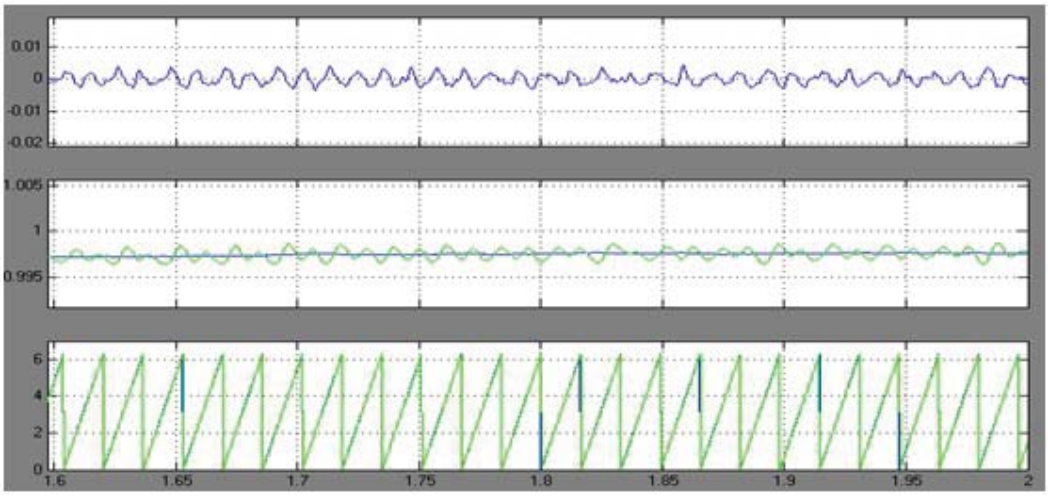

Fig. 4.9. Static actual value and estimated value comparison

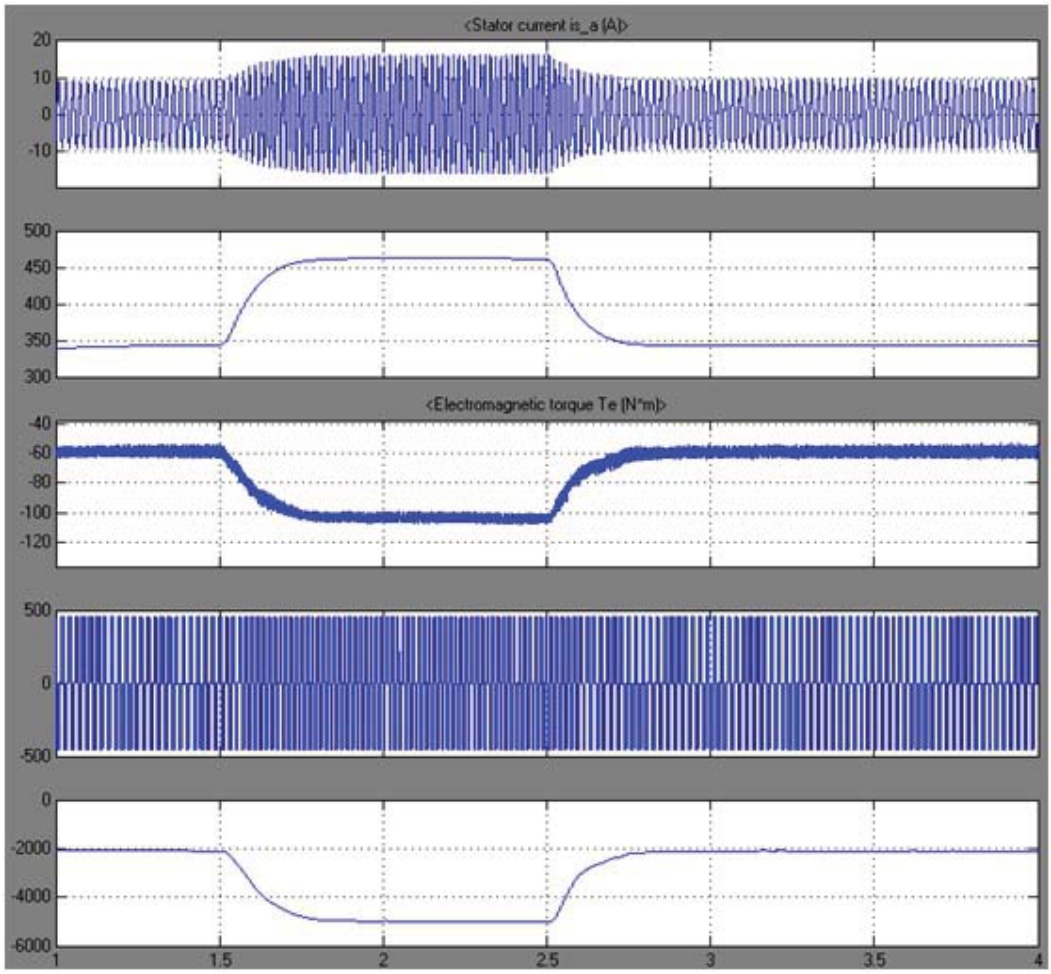

Fig. 4.10. Dynamic characteristic of speed sensorless control

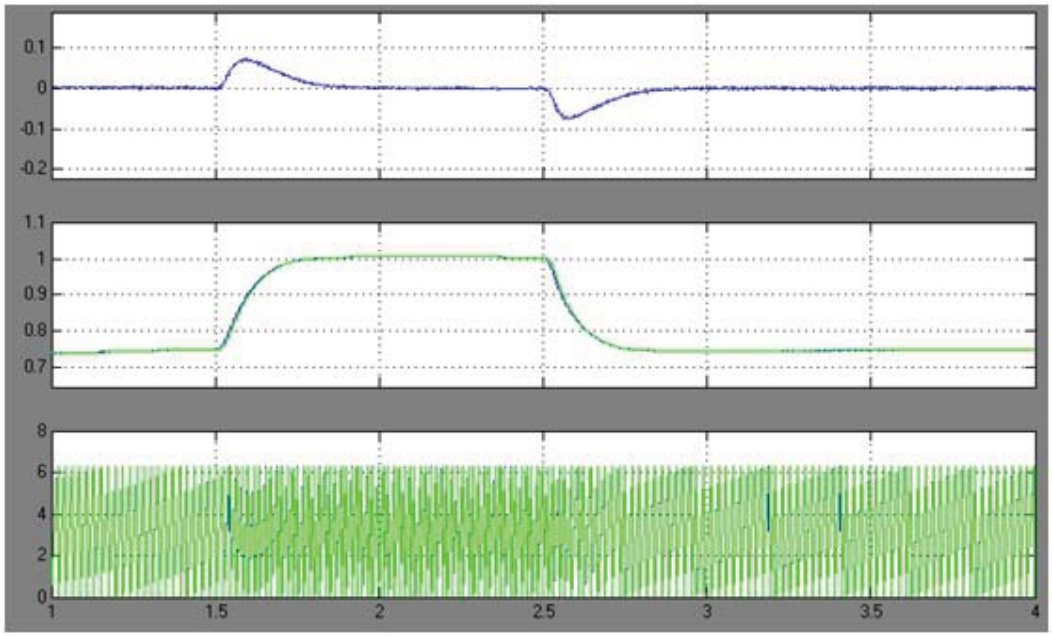

Fig. 4.11. Rotor position, actual rotation speed and estimated rotation speed

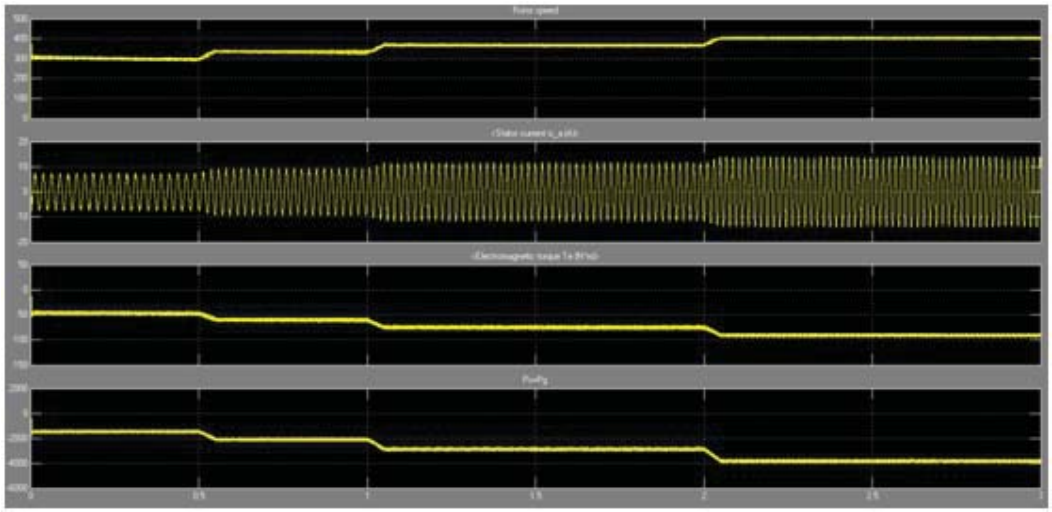

Fig. 4.12. HCM simulation result

5. CONCLUSION

In this thesis, wind power system simulation model was established by using a 5 KW permanent magnet synchronous generator. Rotor flux field orientation vector control method was chosen to develop the model. By using this model, three control methods were applied: the tip speed ratio control, the speed sensorless control and the fuzzy based hill climbing method control.

TSR control was first applied. Based on TSR control, speed sensorless method used estimate rotor position and rotation speed instead of actual measured value to avoid the usage of speed sensor. Compared the simulation results of TSR control and speed sensorless control, the static and dynamic characteristics showed that the performance was almost the same.

At last, a new fuzzy based hill climbing method was applied on the model. Adaptive searching steps were provided by fuzzy system for maximum power peak searching. As the power VS wind speed curves were the combination of hyperbolic curves and parabola curves, small step was used when the gradient was large and large step was chosen when the gradient was small. In order to simplify the fuzzy rule design, Δp and Δwe was applied and the optimize speed can also increase. Sign followed rules to decide whether go uphill or go downhill. In simulation, the power followed the wind change faster than TSR control, especially when the operation point was far from the peak power. When the operation point got close to the peak power, the response time was a little longer than using the TSR control. However, the time was still acceptable.

6. FUTURE WORK

Generally, two works would be done in the future. On one hand, intelligent algorithm may apply to optimize the fuzzy system. On the other hand, besides the maximum power tracking, the maximum power limit control could be done so that a complete power control system is built.

6.1 Algorithm Optimization

In addition to TSR control, speed sensorless control and fuzzy based hill climbing method that used in the project. Other intelligent control methods, such as neutral network may also conquer the wind power's nonlinearity and complexity and provide similar or ever better performance. These kinds of methods can be applied and compared to find the better control strategy.

In fuzzy based hill climbing method, the fuzzy domains and membership functions are set manual, mainly based on lookup table. The ranges and rules are generally decided by the summarized discipline of the collected datum. Several advanced control method, such as PSO or genetic algorithm could be applied to optimize the rules and the ranges so that the performance would elevate.

6.2 Maximum Power Limit

Maximum power control has two parts, the maximum power point tracking (MPPT) and the maximum power limit (MPL). This thesis focus on MPPT, however, the control strategy may expand for MPL.

The MPL strategy includes two parts, the constant power district judge and the constant power district control strategy.

The constant power district judge is the premise of MPL control. When the rotation speed exceeds the generator's rated rotation speed, the output power surpasses the rated power. Consider the safety request, the current is also used as a judge criteria. If the system passes the limit line, the stator current should be reduced to proper value to keep the system constantly output power at 5 KW.

LIST OF REFERENCES

LIST OF REFERENCES

[1] Y. Chen, Y. He, Y. Bao, and J. Shen, "Present situation and future development of wind power in china," pp. 1664–1667, Industrial Electronics and Applications, 2008. ICIEA 2008. 3rd IEEE Conference on, 2008.

[2] W. Head, "World wind energy report 2009," tech. rep., 2009.

[3] W. Head, "World wind energy report 2010," 2010.

[4] D. Li and L. Niu, "Reliability analysis of electric distribution system integrated with wind power," pp. 729–733, Industrial Electronics and Applications, 2008. ICIEA 2008. 3rd IEEE, 2008.

[5] T. Ackermann and L. Soder, "An overview of wind energy-status 2002," *Renewable and Sustainable Energy Reviews*, vol. 6, no. 1-2, pp. 67–127, 2002.

[6] M. Gu, "Research on strategic importance of non-grid-connected wind power for us energy development," pp. 1–5, Decision and Control, 2009 held jointly with the 2009 28th Chinese Control Conference. CDC/CCC 2009. Proceedings of the 48th IEEE Conference on, 2009.

[7] G. Joselin Herbert, S. Iniyan, E. Sreevalsan, and S. Rajapandian, "A review of wind energy technologies," *Renewable and Sustainable Energy Reviews*, vol. 11, no. 6, pp. 1117–1145, 2007.

[8] S. Calvert, R. Thresher, S. Hock, A. Laxson, and B. Smith, "Us department of energy wind energy research program for low wind speed technology of the future," *Journal of solar energy engineering*, vol. 124, p. 455, 2002.

[9] S. Thor and P. Weis Taylor, "Long term research and development needs for wind energy for the time frame 2000-2020," *Wind Energy*, vol. 5, no. 1, pp. 73–75, 2002.

[10] A. Chertok, D. Hablanian, and P. McTaggart, "Development of a direct drive permanent magnet generator for small wind turbines," tech. rep., TIAX LLC, Cambridge, MA, 2004.

[11] F. Bianchi, H. De Battista, and R. Mantz, *Wind turbine control systems*. Springer-Verlag London Limited, 2007.

[12] K. Tan and S. Islam, "Optimum control strategies in energy conversion of pmsg wind turbine system without mechanical sensors," *Energy Conversion, IEEE Transactions on*, vol. 19, no. 2, pp. 392–399, 2004.

[13] R. Krishnan, *Electric motor drives: modeling, analysis, and control*, vol. 58. Prentice Hall, 2001.

[14] J. Manwell, J. McGowan, and A. Rogers, *Wind energy explained: theory, design and application*. John Wiley Sons Inc, 2010.

[15] T. Ahmed, K. Nishida, and M. Nakaoka, "Mppt control algorithm for grid integration of variable speed wind energy conversion system," pp. 645–650, Industrial Electronics, 2009. IECON '09. 35th Annual Conference of IEEE, 2009.

[16] B. Neammanee, S. Sirisumranukul, and S. Chatratana, "Control performance analysis of feedforward and maximum peak power tracking for small-and medium-sized fixed pitch wind turbines," pp. 1–7, Control, Automation, Robotics and Vision, 2006. ICARCV '06. 9th International Conference on, 2006.

[17] D. Liu, Z. Wu, H. Wang, and T. Wang, "Mppt control strategy for off-grid wind power system," pp. 759–764, Power Electronics for Distributed Generation Systems (PEDG), 2010 2nd IEEE International Symposium on, 2010.

[18] R. Karki and P. Hu, "Wind power simulation model for reliability evaluation," pp. 541–544, Electrical and Computer Engineering, 2005. Canadian Conference on, 2005.

[19] D. Ohm, "Dynamic model of induction motors for vector control," *Drivetech, Inc., Blacksburg, Virginia*, 2001.

[20] G. Ramtharan, N. Jenkins, and O. Anaya Lara, "Modelling and control of synchronous generators for wide range variable speed wind turbines," *Wind Energy*, vol. 10, no. 3, pp. 231–246, 2007.

[21] B. Neammanee, K. Krajangpan, S. Sirisumrannukul, and S. Chatrattana, "Maximum peak power tracking-based control algorithms with stall regulation for optimal wind energy capture," pp. 1424–1430, Power Conversion Conference - Nagoya, 2007. PCC '07, 2007.

[22] R. Datta and V. Ranganathan, "A method of tracking the peak power points for a variable speed wind energy conversion system," *Energy Conversion, IEEE Transactions on*, vol. 18, no. 1, pp. 163–168, 2003.

[23] L. Fan, Z. Miao, and X. Wang, "Sensorless maximum power point tracking in multi-type wind energy conversion systems," pp. 6823–6828, IEEE, 2009.

[24] R. Esmaili, L. Xu, and D. Nichols, "A new control method of permanent magnet generator for maximum power tracking in wind turbine application," pp. 2090–2095 Vol. 3, Power Engineering Society General Meeting, 2005. IEEE, 2005.

[25] K. Raza, H. Goto, H. Guo, and O. Ichinokura, "A novel speed-sensorless adaptive hill climbing algorithm for fast and efficient maximum power point tracking of wind energy conversion systems," pp. 628–633, Sustainable Energy Technologies, 2008. ICSET 2008. IEEE International Conference on, 2008.

[26] M. Simoes, B. Bose, and R. Spiegel, "Fuzzy logic based intelligent control of a variable speed cage machine wind generation system," *Power Electronics, IEEE Transactions on*, vol. 12, no. 1, pp. 87–95, 1997.